NACA RM A52A18

NACA

RESEARCH MEMORANDUM

INSTRUMENTATION OF THE AMES SUPERSONIC FREE-FLIGHT WIND TUNNEL

By Robert O. Briggs, William J. Kerwin, and Stanley F. Schmidt

Ames Aeronautical Laboratory
Moffett Field, Calif.

NATIONAL ADVISORY COMMITTEE FOR AERONAUTICS

WASHINGTON

April 24, 1952

NATIONAL ADVISORY COMMITTEE FOR AERONAUTICS

RESEARCH MEMORANDUM

INSTRUMENTATION OF THE AMES SUPERSONIC FREE-FLIGHT WIND TUNNEL

By Robert O. Briggs, William J. Kerwin, and Stanley F. Schmidt

SUMMARY

A description of the equipment used in the Ames supersonic free-flight wind tunnel to obtain the data necessary to measure the aerodynamic characteristics of free-flying models is presented.

The model to be studied is fired from a gun into the supersonic air stream of a blowdown-type wind tunnel. Model motion resulting from aerodynamic forces is computed from a time-distance-attitude record of the model flight through the test section.

Model attitude is determined from shadowgraphs taken at seven stations. The equipment used for time-distance measurements includes four of these shadowgraph stations and a chronograph. Each shadowgraph station consists of a photoelectric model detector which triggers a spark gap, the illumination from which is projected through the test section on to a photographic plate. The position of the model relative to a distance reference scale can be determined from the shadowgraph thereby obtained. A portion of the light from each spark gap is diverted onto the film of a rotating-prism-type chronograph. An accurate time reference is placed on the chronograph film by light pulses of 1 microsecond duration (from a mercury arc lamp) which may be pulsed at rates from 10,000 to 100,000 pulses per second.

The nominal accuracies of the instruments are 0.003 inch for distance measurement and 0.1 microsecond for time measurement. As an indication of the over-all accuracy obtainable in measuring drag, the drag coefficients of 32 cone-cylinder models were measured over a wide range of Mach numbers; the mean scatter of these measurements from a faired curve was 1.2 percent.

Three additional shadowgraph stations which are mounted at right angles to the four previously mentioned provide the additional data necessary to fix the model attitude.

INTRODUCTION

The Ames supersonic free-flight wind tunnel has been developed to study aerodynamic phenomena by a combination of wind-tunnel techniques and conventional ballistic-research techniques. Data are obtained by firing an aerodynamic model from a gun into the supersonic air stream of a blowdown-type wind tunnel and recording the behavior of the model. The Mach number is increased above that obtainable in the ballistic range because of both the added velocity of the supersonic air flow, and the reduced speed of sound due to lowering of the temperature of the air as it expands in the nozzle. Control of the model velocity allows a much wider variation of Mach number than is obtainable in a conventional wind tunnel.

The small, fast, free-flying models which undergo high acceleration during launching and stopping do not lend themselves to internal instrumentation; therefore, all data are measured externally by means of photographic and electronic recording instruments.

This report has been prepared to present a description of the wind-tunnel instrumentation to those interested in the details of its development and construction.

Detailed information on the aerodynamic characteristics of the tunnel, the operation of the tunnel, and the reduction and interpretation of aerodynamic data is presented in reference 1.

GENERAL DESCRIPTION

Most of the instrumentation effort applied to the supersonic free-flight wind tunnel has thus far been directed toward the precise measurement of time per unit distance as the model traverses the test section. The records obtained are used to compute the deceleration of the model (which is a result of the drag force on the model), and thus to study the drag forces involved. The results of some of these measurements are discussed in reference 1.

The physical arrangement of the tunnel may be seen in figure 1. Figure 2 is a photograph of the test chamber of the tunnel. Supersonic

flow is established by the nozzle shown at the left of figure 1 and is maintained uniform throughout the 18-foot length of test section. The model launching gun appears at the right. The Invar frame suspended from shock mounts in the pit below the test section supports the optical components associated with the time-distance measuring equipment. The primary purposes of the frame are to provide isolation from tunnel vibration, and to keep to a minimum changes in alinement resulting from temperature variation.

A simplified drawing of the test section and optical assembly is presented in figure 3. Four vertical shadowgraph stations are provided as shown on this drawing. At each shadowgraph station a flash of light is obtained from a spark discharge triggered while the model is in the field of view. The shadowgraphs obtained at these stations show the position of the model at the instant of the flash relative to a fixed Invar scale, allowing the distance traversed by the model between shadowgraph exposures to be precisely determined.

The time interval between successive shadowgraph exposures is measured by means of a photographically recording chronograph. The chronograph diverts some of the light from each shadowgraph light source and focuses it through a rotating prism onto a strip of film 15 feet in length. This film lines a circular track which is concentric with the axis of rotation of the prism. Four spots resulting from these exposures are distributed around the film with a spacing dependent upon the rate of rotation of the prism and the time interval between shadowgraph exposures.

Time reference marks are placed on the chronograph film by light from a pulsed mercury arc lamp. The interval between pulses is determined by a crystal-controlled frequency standard. Rates of 10,000, 20,000, 50,000, and 100,000 pulses per second may be selected as required by the test.

A data run consists of a 15-foot flight of the model through the test section during which the four shadowgraphs are taken and a 15-foot chronograph film record is made.

Sequence of Operations During a Data Run

A knowledge of the chronological sequence of operations during a data run is helpful in understanding the instrumentation of the wind tunnel and is presented below.

Before the run is begun, the rotating prism is adjusted to a speed such that it will make slightly less than one complete revolution in the time required for the model to traverse the test section. The run is initiated by preheating the pulsed mercury arc lamp to obtain optimum light intensity. A photoelectric monitoring circuit observes the pulsed light and fires the gun when the pulsed light intensity reaches a

predetermined value. A capping shutter on the film drum is opened simultaneously with the firing of the gun.

Photoelectric model detectors (called photobeams) which respond to the interruption of light beams by the model, control the succeeding operations. As the model enters the test section of the tunnel, a rapid acting shutter, known as the optical gate, opens admitting the light from the pulsed mercury arc lamp through the rotating prism onto the film where each successive pulse is recorded as a comet shaped mark. At a predetermined time after the interruption of the No. 1 photobeam, the shadowgraph light source at station No. 1 flashes illuminating the model (which has moved to the center of the field during the time delay) and providing a station mark on the chronograph film.

The model progresses down the test section with shadowgraphs being similarly taken at stations 2, 3, and 4 and is finally caught by the model catcher. (The force of impact usually destroys the model.) The pulsed lamp is automatically extinguished after the last shadowgraph is taken. Some time later the capping shutter and optical gate close.

A section of a chronograph record is shown in figure 4(a). The uniformly spaced, comet shaped spots are time reference marks recorded at 50,000 pulses per second. The additional spot near the middle of the record is the station mark corresponding to the instant at which the model was shadowgraphed at a station. A typical shadowgraph is shown in figure 4(b). The distance reference scale appears along the top edge.

THE SHADOWGRAPH EQUIPMENT

The shadowgraph equipment used is essentially the same as that used by most ballistics ranges.

Physical Arrangement

The physical arrangement of the shadowgraph equipment is illustrated in figure 3. This figure shows stations 1, 2, 3, and 4 which obtain shadowgraphs of the vertical projection of the model, but does not show side stations (5, 6, and 7) which obtain shadowgraphs of the horizontal projection of the model.

Side stations 5 and 7 are operated simultaneously with vertical stations 1 and 4, respectively, and obtain shadowgraphs of the same field as the corresponding vertical stations, except at right angles

thereto. Side station 6 is located midway between vertical stations 2 and 3.

Shadowgraph Light Source

The necessary high-intensity, short-duration point source of light is obtained by discharging 1.6 watt-seconds of energy from a 0.1 microfarad condenser, initially charged to 6000 volts, through a tertiary spark gap at atmospheric pressure. A photograph of the spark gap is shown in figure 5(a) and a cutaway drawing is shown in figure 5(b). The ground and high-voltage electrodes are aluminum, and the trigger electrode is of tungsten. Light is projected along the high-voltage electrode axis through a 0.040-inch-diameter aperture. Light for the chronograph is obtained through a 1/4-inch aperture in the side of the spark housing. The effective duration of the light flash is approximately 0.3 microsecond. The spectral distribution of the photographically effective light is illustrated in figure 6. The wave lengths in angstrom units of the most prominent lines and the associated chemical element are indicated. Relative exposure times were 1, 4, 16, and 64, respectively.

Optical System

The discussion of the optical system of the shadowgraph equipment considers only one station, as all stations are optically identical. The 0.04-inch-diameter aperture of the spark gap is small enough to be considered a point source of light in this system.

The spark gap is mounted so that its aperture is located at the focal distance from the spherical collimating mirror, but not on the optical axis of the mirror. This off-axis location is necessary to prevent obstruction of the illuminated field by the spark gap but has the undesirable result of preventing complete collimation of the light, thus causing some distortion in the shadowgraph record. The imperfections in the light beams due to this and other causes, including defects in the mirrors and windows and errors in alinement of the optics, were determined from a calibration which is used in the precise determination of model position.

The nearly parallel light is projected through the test section of the tunnel which is fitted with windows so that all optical components may be located outside the tunnel. An 8- by 10-inch plate holder at the top of the tunnel secures the glass photographic plate in such a position that the light projected through the test section exposes it,

recording a shadow of the model and of the notched distance reference scale. The position of the model can be determined within ±0.003 inch. This limitation in measurement accuracy results from: (1) imperfect calibration of the light beams, including the effect of small movements of the spark gaps and mirrors, (2) distortion caused by boundary layer at the windows, (3) density gradients in the flow, (4) the finite size of the light source, and (5) blur at high model velocities due to the finite duration of the spark.

The Photobeam

In order to fire the spark gap at the proper instant to include the free-flying model in the field, a detector and time-delay system is used.

The model detector, or photobeam, consists of a collimated beam of light, approximately 7 by 1/4 inches in cross section which is projected through the test section from top to bottom and is focused on a phototube. The interruption of the light beam by a model is detected by the phototube and the resultant signal is used to initiate succeeding operations.

The light source for the photobeam is a 12 to 16-volt, 50-candlepower bulb which is operated from a direct-current power supply. Because of mounting and space problems, the lenses used for the photobeams are rectangular segments of 12-inch focal-length plano-convex lenses. One of these lenses and a photobeam-detector chassis appears in figure 7.

The photobeam is located to the gunward side of the shadowgraph. A time delay between the detection of the model and the firing of the spark is therefore necessary in order to place the shadow of the model at the center of the photographic plate.

Undesired exposure of the photographic plate is reduced by the use of a red insensitive emulsion (super orthopress), and a red filter in the photobeam optical system.

Electrical Equipment

The block diagram of the electronic equipment for the four shadowgraph stations is shown in figure 8.

The voltage pulse produced by the phototube upon the interruption of the photobeam is amplified by the preamplifier (which is located on the photobeam-detector chassis) and the amplifier. The positive pulse output of the amplifier initiates the operation of the electronic time-delay circuit which, after the preset time has elapsed, triggers the spark gap.

The interference eliminating circuit was developed to prevent triggering of one spark, by electrical interference with its phototube or preamplifier, when another spark fires. The function of the interference eliminating circuit is to make the amplifiers of all the stations inoperative when any spark is firing. Its use and operation are discussed in more detail later in this report.

Problems resulting from interference.- The majority of problems encountered in the development of the shadowgraph system were the result of spurious signals which triggered the spark gaps at improper times. These spurious signals were studied and classified as follows:

1. Transient electromagnetic interference of one spark gap with the high gain amplifiers of another station

2. Continuous noise developed within the photobeam, preamplifier and amplifier

   a. Noise resulting from vibration of the photobeam light and phototube

   b. Microphonic noise resulting from vibration of the preamplifier

   c. Random noise (Shott effect, etc.) developed in the phototube and preamplifier

The electrical interference between shadowgraph units was the most acute problem presented. The limitations on the physical placement of the various units of the shadowgraph system introduced serious intercoupling possibilities between the spark gaps and the preamplifiers and amplifiers.

Electrical interference was reduced by electrical shielding of spark gaps, cables, and preamplifiers, and electrically isolating the spark-gap high-voltage cable from the spark gap by means of a resistance-capacitance network, thereby preventing cable radiation. These additions, although changing the manner of occurrence and reducing the frequency of interferences, were still not sufficient to make the system usable under all conditions.

One of the alternatives suggested was to allow the interference to occur as it might, but to paralyze the amplifier circuits of all units for a short time during the firing of a spark, so that even though energy transfer occurred, no other spark could be triggered thereby. This was accomplished by use of the interference-eliminating circuit which, 25 microseconds preceding the firing of any spark gap, delivers a 200-volt negative pulse to the screen grid of one of the amplifier tubes of each of the units, preventing the tube from amplifying any signal appearing at its grid for the 300-microsecond duration of the negative pulse.

The second classification of interference differs from the first in that its occurrence is continuous, and its amplitude lower.

Noise resulting from the change in incident energy on the phototube when any of the optical components of the photobeam vibrate was reduced by diffusing the light before it reached the phototube.

Microphonic noise was reduced by shock mounting the photobeam-detector chassis. The microphonic noise (the majority of which is below 5000 cycles per second) was further reduced by attenuating the low frequency response of the preamplifier. The remaining noise is rejected by biasing the grid of a control tube past cut-off by a voltage slightly greater than the peak noise level. The bias is adjusted to give optimum signal to noise ratio under the noisiest tunnel operating condition.

Electronic circuit description.- The schematic diagram of the electronic circuit for one shadowgraph station, including the interference eliminator common to all stations, is shown in figure 9. Power supplies are not shown.

The preamplifier for the phototube V1 consists of a resistance-coupled voltage amplifier V2 and V3 coupled to the low-impedance output cable by a cathode follower V4. The output of the preamplifier is about 40 volts for the smallest model tested to date (0.2-inch diameter, 0.4-inch length). When V5 is not paralyzed by the interference eliminating circuit, and a positive signal of magnitude great enough to exceed the bias on the grid is delivered from the preamplifier, the signal is amplified by V5 and V6 and applied to the grid of the thyratron V7. This positive pulse output of V6 from station 1 is also used to initiate the operation of the optical gate. The thyratron V7 is fired by the positive pulse applied to its grid, initiating the charging of the capacitor C16 (or C16 and C15 depending upon the position of the range switch) via V7 and R24 from the regulated 300-volt, d-c. supply. The time required to charge the condenser to the firing potential of thyratron V8 determines the delay introduced by the circuit This time is variable by either changing the capacitance with the range

switch or by varying the quiescent voltage on the grid of V8 which is adjustable by potentiometer P3.

The voltmeter, VM, is used to set the bias for any desired delay. Range 1 covers 40 to 400 microseconds and range 2 covers 400 to 4000 microseconds. When V8 fires, capacitors C18 and C19 are discharged through the primaries of the two ignition coils T1 and T2, the secondaries of which are coupled to the trigger electrodes of the vertical and side shadowgraph spark gaps. A delay of approximately 25 microseconds occurs between the firing of V8 and the firing of the spark gap. Most of the delay results from the relatively long rise time of the secondary voltage of the ignition coil.

The interference eliminating circuit consists of a single shot multivibrator V10 which is triggered by the negative pulse derived from the differentiated output of thyratron V8. This negative pulse is delivered to the multivibrator from all units by a common conductor. A 300-microsecond pulse output of the multivibrator is amplified by V9. The application of the 200-volt negative signal from V9 to the screen grid of V5 reduces the gain of V5 to zero.

The interference elimination pulse is initiated simultaneously with the exciting of the primary of the trigger coil. The delay of approximately 25 microseconds in the firing of the spark gap after excitation of the primary of the trigger coil insures that the 200-volt pulse will be applied to the screen of V5 by the time the spark gap fires since the rise time of the interference eliminating pulse is 7 microseconds.

The 300-microsecond duration of the interference eliminating pulse is long enough that all interfering signals have diminished before its removal, but short enough so that the circuits are always operative before the arrival of the model at the next station.

THE CHRONOGRAPH

It was decided early in the planning of the supersonic free-flight wind tunnel that a rotating-prism-type chronograph with an accurate time base would provide a more absolute measure of time than would any of several electronic chronographs which were proposed. The intervals to be measured were from 2000- to 20,000-microseconds duration with a desired definition of 0.1 microsecond or less. The relative ease of computing light signal transit times, of measuring optical distortions, and the supposed lack of critical components of the rotating-prism system made it seem preferable to an electronic system in which electrical delays might not be constant or circuits might perform erratically.

For these reasons, a rotating-prism chronograph was designed for obtaining time data and for use as a standard against which to check any other chronograph which might be added at a later date.

Optical System

The chronograph optical system, shown in figure 3, provides an image of each shadowgraph light source and of the pulsed mercury arc lamp at the 0.03-inch-diameter aperture of the optical gate. This is accomplished by the concentric mirror and lens assembly shown in figure 10. An image of this aperture is focused through the 90° prism onto the film which lines the 188-inch circumference of the film drum. Coated achromatic lenses are used throughout.

The capping shutter (a Betax 5) located immediately above the film drum, opens when the gun is fired and closes 1 second later.

The prism consists of a quartz cylinder split diagonally in two halves and silvered at the junction. It is mounted in a steel setting which is attached directly to the drive motor shaft. Figure 11 is a photograph of the prism and drive motor. The induction-type motor, powered by a variable-frequency motor-generator set, drives the prism at any desired rate from 0 to 24,000 revolutions per minute. Fundamental mechanical resonance occurs at 7200 rpm necessitating that operation at this rate of rotation be avoided. The rate of rotation of the prism (determined by the calculated model velocity) is usually set so that the prism will make slightly less than one complete revolution during the calculated time required for the model to traverse the test section. Eighty to ninety percent of the 188-inch length of film is allowed for use in the majority of data runs.

A Mitchel 500-foot hand-wound film magazine is mounted on the side of the film drum to allow loading and unloading of the film. The felt seals on the magazine film slots had to be removed to prevent static charging of the film and resultant exposure due to spark breakdown. Film stickage in the drum is prevented by carefully polishing and chrome plating the brass strips against which the film bears.

The mechanics of leading the film into and out of the film drum leaves a 1-inch section without film. A small projector not shown in figure 3 marks the lead-in and lead-out points on the film so that any timing marks which might have fallen on this section may be interpolated from the other timing marks. If, however, a station mark should fall in this section, it is lost. Since each run normally contains four station marks the probability of loss of one of these is 1 in 47. The projector previously mentioned also places identifying numbers on the chronograph film.

The Pulsed-Light Time Reference

Experiments with the kerr cell.- A kerr cell (reference 2) used in conjunction with a high-intensity light source was originally considered as a means of obtaining pulsed light for placing timing marks on the chronograph film. An experimental setup was made to pulse the kerr cell at rates of from 40 to 100,000 pulses per second. This equipment was completed before the rotating-prism assembly was available for experimental use; however, tests were conducted using a phototube and an oscilloscope to plot light intensity versus time, and a ratio of peak intensity transmitted by the kerr cell to source intensity was determined. The maximum light transmission obtainable from the kerr cell was found to be 20 percent of the incident intensity. Calculations showed that several times more light would be required than was available with the kerr cell optical system as planned. Therefore, the following alternative techniques were considered in order to increase the pulsed-light intensity at the film: (1) redesign the optical system; (2) obtain a more intense steady-state light source than was then available (the BH-6, the Ames type A, or the Ames type B mercury arc lamps, reference 3); or (3) directly pulse a high-intensity lamp to obtain a much higher peak intensity than average steady-state intensity, and thereby also eliminate the losses inherent in the kerr cell. Alternative (3) was chosen because it was the only method that held promise of increasing the light by the amount necessary.

Preliminary investigation of a directly pulsed lamp.- Light is produced in a gas discharge lamp by atoms of the gas undergoing a change in energy level (reference 4). The atoms will absorb energy when excited to a higher level and release it as light when reverting to their normal state.

The duration of the radiation produced by a gas-discharge lamp after the removal of the exciting electrical impulse is determined by the time required for the excited atoms of the gas to return to their normal state.

The excited state duration τ is defined by the following equation:

$$\tau = t \log_e \frac{N}{N_o}$$

where

N_o the number of excited atoms at time $t = 0$, which is the time of removal of excitation

N the number of excited atoms at time t

For most normal transitions in the mercury atom an experimentally determined value of τ is approximately 10^{-8} seconds, thus for a decay to 1/e of the number of initially excited atoms t equals 10^{-8} seconds, or 0.01 microsecond.

Some of the transitions in the mercury atom do exhibit a longer duration. One of the longest times, that of the transition from 6^3P_1 to 6^1S_0 (the 2536 angstrom line) is 10^{-7} seconds. In addition there are forbidden transitions in which meta-stable atomic states may exist, giving possible excited state durations as long as 10^{-2} seconds; fortunately, however, the number of atoms excited to meta-stable states is relatively small. When a mercury arc lamp is excited by a short duration electrical pulse, the total time of light emission is therefore no greater than the sum of the exciting pulse duration and τ, and pulsing at rates up to at least the desired 100,000 per second should be possible.

Consequently, the pulsing circuit which had been used to operate the kerr cell was modified to be used for the experimental pulsing operation of a BH-6 mercury arc lamp.

The BH-6 mercury arc lamp is a two-electrode capillary-type lamp with an electrode spacing of 25 mm, an outer diameter of 6 mm, and a capillary diameter of 2 mm. It is designed for use with air cooling which is provided by means of two air jets impinging on the outer surface of the quartz capillary tube opposite the electrode tips. The normal continuous power consumption of the lamp is 900 watts (900 volts at 1 ampere d-c.). Under these conditions, and with normal cooling, the internal pressure of the lamp is 120 atmospheres and its impedance is approximately 900 ohms. The impedance of the lamp when cold is approximately 10 ohms.

Pulse operation of the lamp was accomplished by driving it with a pulsed voltage of 7,000 to 10,000 volts peak having the desired repetition rate and pulse width. It was found that pulsed light could be generated in this way having a pulse width (after a decay to 1/e of the peak intensity) of less than 1 microsecond and a peak intensity of many times the average intensity under rated conditions.

Development of the Pulsed-Lamp Technique

Three major problems were encountered in development of the pulsed-lamp technique. These problems were at first treated separately, but it was found that conditions affecting one problem would affect the others. The solutions of the problems were, therefore, closely interrelated.

Preheating problem.- In order that the lamp produce the required light output for exposure of the chronograph film during a data run, a process of preheating is required. The most satisfactory procedure for preheating is to supply the lamp with rated d-c. power and air cooling for 15 seconds after which pulse power is applied and air cooling removed. The internal temperature of the lamp and the intensity of the pulsed light from the lamp increase as the preheating proceeds. Two systems of terminating the pulse preheat at the proper instant were tested. The first system was the use of a fixed timing device. This was not successful since the time necessary for the light output of the lamp to reach the required intensity is not constant. The second system was the use of a circuit to automatically terminate the pulse preheat when the output of a phototube monitoring circuit reached a predetermined value.

Restarting problem.- In the first attempt to utilize the pulsed lamp in the chronograph (prior to installation of the optical gate), it was necessary to extinguish the lamp when it had been preheated sufficiently, after which the gun was fired and the capping shutter opened. The lamp was then restarted by reapplying pulse voltage at the instant the model entered the test section, and remained on for the period during which data was recorded. When the BH-6 lamp is heated so that sufficient intensity is obtained to expose the chronograph film its temperature is very near and sometimes in excess of a critical temperature above which the lamp, if extinguished, will not restart upon the application of pulse voltage. Failure of the lamp to restart resulted in records in which part or all of the chronograph film was without timing marks. This occurred frequently.

Modifications of the preheat and operating sequence in an attempt to correct the late restarting problem were only slightly successful. A reduction in the operating temperature was not practicable, especially in view of the flicker problem discussed later, the solution of which necessitated even higher operating temperatures. The final solution was to eliminate the necessity for stopping and restarting the lamp by inserting a rapid-acting shutter in the optical path. The operation of this shutter is discussed in a later paragraph.

Flicker problem.- A series of photographs, taken with the rotating-prism equipment, of the arc within the BH-6 lamp under pulse operation at 100,000 pulses per second is presented in figure 12. This figure illustrates the phenomenon of flicker which was another problem encountered. The peculiar inconsistency of the shape and position of the arc within the capillary from instant to instant always occurs under pulse operation. It becomes more pronounced at high intensities and high pulse rates.

In the chronograph an image of the mercury arc must be focused on the 0.030-inch-diameter aperture. An image of this aperture is focused on the chronograph film and forms a timing mark each time the lamp is pulsed. The light intensity as observed through this aperture varies as the image moves onto or away from the center of the aperture. This variation, called flicker, causes a change in the density and shape of the timing marks from pulse to pulse which lead to uncertainties in the time measurement.

The lamp was placed at the center of a cylindrical mirror which focuses a reversed image of the arc in the plane of the real arc so that when the real arc moves in one direction the image moves in the opposite direction, thereby tending to maintain uniform illumination over the entire aperture. The amount of flicker was thereby reduced but was still objectionable. Frosting the outside surface of the aperture side of the lamp, thereby diffusing the light, eliminated the remaining flicker. The loss of intensity resultant from diffusing the light necessitated operating the lamp at higher intensity than was otherwise required, placing the operating temperature well above the critical temperature for restarting. This higher operating temperature aggravated the restarting problem which, as previously mentioned, was solved by eliminating the necessity for stopping and restarting a hot lamp.

Rapid Acting Shutter, or Optical Gate

The operation of the rapid-acting shutter (which was called the optical gate to distinguish it from the capping shutter) is to prevent light from reaching the rotating prism until the model reaches the test section. It then opens and remains open until completion of the run. The optical gate is designed to open in less than 100 microseconds. This allows the initiating signal to be taken from the No. 1 photobeam since it is interrupted at least 100 microseconds before the first shadowgraph is taken. The optical gate, which is illustrated in figure 13, is an electromechanical device designed so that a minimum of mass is moved in order to uncover the aperture. The cylindrical magnet is designed to concentrate the flux in the pole gap, very little external leakage being permitted. The current through the 20,000 turns of No. 28 wire provides a magneto-motive force of 2,000 ampere turns which establishes a field of approximately 8,000 gausses between the pole pieces. The only moving parts are the armature assembly and the coil spring suspension. The armature assembly consists of a single wire with a paper disc at its center and a small mass load at the ends. Discharging an 80-microfarad condenser (initially charged to 200 volts) through the wire causes it to move perpendicularly to the magnetic field, removing the paper disc from the light path which is axial with the magnetic field.

In order that the optical gate comply with the two major design criteria of opening in less than 100 microseconds and of staying open for 20,000 microseconds, the design of the coil spring suspension and armature assembly required careful consideration. The coil spring suspension provides high compliance to the motion of the armature. The combination of the compliance and the mass loading results in a resonant period of 40,000 microseconds. The mass loading does not appreciably increase the opening time as the wire bows on the application of the initial force, thus opening the aperture before the weighted ends are moved appreciably. Opening times of 70 microseconds are obtained with this optical gate.

The use of the optical gate to permit reliable operation of the pulsed mercury arc lamp with the rotating-prism chronograph is completely successful.

Electronic Components

General description.- Figure 14 is a block diagram of the electronic components associated with the chronograph. A data run is initiated by closing the firing key which energizes the d-c. preheat timing control. The d-c. preheat timing control causes the d-c. switching relay to close, applying the full output of the d-c. preheat power supply and normal air cooling to the lamp for the predetermined time of approximately 15 seconds. At the termination of this time, the preheat relay opens, removing the preheat voltage from the lamp and sending a signal to the start terminal of the pulse and the d-c. gate. Input to the pulse gate is supplied from the pulse generator which is synchronized with the frequency standard. Pulse operation of the lamp proceeds as previously described until the intensity of the lamp (as measured by the preheat monitor) reaches the required value. The preheat monitor then actuates the firing relay which is interlocked with the firing key to prevent accidental firing of the gun. The firing relay simultaneously fires the gun and opens the capping shutter. The optical-gate control receives its initiating signal from the interruption of the first photobeam. The pulse and d-c. gates receive their stop signal from spark gap number 4.

The firing key and all switches and meters necessary to monitor and control the data run are located at a central switchboard.

The present installation of the electronic equipment associated with the chronograph is shown in figure 15.

Frequency standard and pulse generator.- A 100-kilocycle crystal-controlled frequency standard is used to synchronize a multivibrator

pulse generator at rates of 10,000, 20,000, 50,000, or 100,000 pulses per second. A switch is used to select the pulse rate and the pulse width which has been preset at optimum for each pulse rate. The 100-volt positive output from the pulse generator is coupled to the gating circuit.

Gating circuit.- The function of turning on or off the d-c. preheat, d-c. keeper, and pulse voltages to the lamp at the proper instants during a data run is performed by the gating circuit. Figure 16 is the schematic diagram of the gating circuit. The d-c. preheat and keeper voltages are controlled by relay RY2. When RY2 is energized to preheat the lamp the positive terminal of the preheat power supply is connected to ground and the negative terminal is connected to the lamp via R19 and R20 which are then in parallel. When RY2 is de-energized the negative terminal of the 1-kilovolt power supply is then connected to the lamp via R20 only and the positive terminal is connected to the plate of V6, the cathode of which is returned through a 100-volt, low-impedance power supply and R18 to ground. The tube V6 is normally biased to cut-off by the 100-volt power supply, thus keeper current does not flow unless the grid of V6 is made positive.

Control of the drive to the pulse amplifier and consequently of the pulse voltage delivered to the lamp is accomplished by the 5881 pulse gating tube, V4. The grid of V4 is driven by the output of the pulse generator. Pulse output from the gating circuit is produced only when the screen grid of V4 is positive.

The screen voltage of V4 and the grid voltage of V6 are applied by firing the thyratron V3 and removed by firing the thyratron V2.

A time delay of 75 microseconds between the receival of a signal to the stop terminal and the removal of the drive to the lamp is obtained by the addition of thyratron V1. This delay allows one or two timing marks to be placed on the chronograph record after the last station mark has been recorded.

In order to insure immediate ionization of the mercury in the lamp upon the closing of relay RY2 and RY1, high-voltage pulses from the pulse amplifier are momentarily applied to the lamp. This is accomplished by placing a positive voltage on the screen of V4 during the time required to charge C13. When the d-c. preheat is terminated by de-energizing RY2 and RY1, the voltage on C13 triggers the thyratron V3, initiating pulse operation of the lamp.

Pulse-amplifier circuit.- The essential components of the pulse-amplifier circuit are shown in figure 17. Figure 18 is a photograph of the pulse-amplifier chassis.

The 300-volt negative pulse output from the pulse gating circuit is connected to the input terminal of the pulse amplifier. The input pulse amplitude on the grid of V2 (an 814 power pentode) is sufficient to drive V2 from zero bias to cut-off. The plate supply voltage of V2 is 1500 volts. A quiescent plate current of 125 milliamperes through the 10,000-ohm plate resistor drops the voltage at the plate to 250 resulting in a plate dissipation of 31 watts.

The final pulse amplifier consists of two 4-250A's, V3, and V4, which are operated in parallel. The 500-volt positive pulse output of V2 drives the grids of the final pulse amplifier from cut-off to 100 volts positive under typical operating conditions. Plate current is supplied from a 10,000-volt source through the 5,000-ohm plate resistor R6 and the 2.5-millihenry peaking coil L2.

The amplifier delivers a peak pulse voltage of about 7,000 volts to the mercury arc lamp. The pulse width (determined by the pulse generator) is preset for each pulse repetition rate so that the average power delivered to the lamp at all rates is about the same. The widths used are: 0.7 microsecond at 100,000 pulses per second; 1.5 microseconds at 50,000 pulses per second; and 4 microseconds at 20,000 and 10,000 pulses per second. Although the instantaneous peak power delivered to the lamp is approximately 14,000 watts, the average power is less than 1,000 watts.

The diode V5 functions as a d-c. restorer and line reflection damper, preventing distortion of the light pulse shape.

The d-c. preheat and the keeper voltages are applied to the lamp through a low-pass filter which isolates the pulse energy from the d-c. supply and gating circuit.

Other pulse amplifying circuits including a plate coupled triode and a cathode follower were tested but the most satisfactory results were obtained with the circuit described.

Accuracy of the Chronograph

The time definition of the rotating-prism chronograph is to within 0.1 microsecond; that is, repeated readings of a given time interval by the same or different individuals will normally agree within 0.1 microsecond. Since no known systematic errors are involved, this figure is also believed to be indicative of the accuracy of the chronograph. This belief is strengthened by the repeatability with which drag coefficient can be measured in cases where time accuracy of this order of magnitude is required. It is also borne out by a comparison with the

time-interval measurements obtained by an electronic chronograph presently being developed and the operation of which is briefly discussed in the appendix.

In a comparison of results of 20 tests wherein records of both the electronic chronograph and the rotating-prism chronograph were taken, an agreement of ±0.1 microsecond was obtained. The accuracy of the electronic chronograph is believed to be 0.05 microsecond.

The first records obtained with the rotating-prism chronograph were in error by 1 microsecond or more. A number of contributing causes were found for this inaccuracy. Among the most important of these were: (1) Flicker was troublesome and was corrected as discussed previously. The result of flicker is to change the shape, size, and intensity of successive timing marks, making it difficult to measure the interval between successive marks. (2) The photographic image was poorly focused, even though the visually observed image was in sharp focus. This was due to the difference between the spectral response of the film and the eye and the use of an uncorrected objective lens. Optimum photographic focus was obtained with the lens 3/16 inch from the position as determined visually. (3) The objective lens was found to be defective, causing distortion of the image. (4) The density of exposure of the film was found to be critical in determining the accuracy with which the record could be interpreted. This was extremely troublesome during the first experimental operation in that the intensity of the pulsed light could not be accurately controlled. Trouble from this cause was reduced by use of the photoelectric monitoring and firing control circuit. (5) Vibration of the optical components of the chronograph was believed to be responsible for some inaccuracy. The vibration was reduced by more careful balance of the prism and motor and changes in the shock mounting of the frame.

During the experimental phases of development of the chronograph, the pulsed-light source was frequently suspected of causing errors in the record. This was natural since less experience was available with the pulsed-light source than with most of the other components. A number of tests were made upon the pulsed light to prove that the intervals between pulses were equal. A phototube and oscilloscope were used in some of these tests and the uniformity of the intervals was established thereby to within 0.01 microsecond.

Interpreting the chronograph records presented a number of problems. It was found that a greater accuracy could be obtained by measuring to the leading edge of the mark than to any other point. The measurement is made by projecting the image to 10 diameters and visually estimating the position of the leading edge with respect to a reticle. This was found to be more accurate than making the measurement with a comparitor densitometer.

Some difficulties are encountered in interpreting records wherein a station mark and a timing mark coincide. The probability of such coincidence depends upon the spacing of timing marks on the film, which varies from 3/8 inch to 1 inch. The position of a station mark can sometimes be determined despite coincidence, particularly if the timing marks are not extremely dense. In one series of 86 runs coincidence reduced the accuracy in only three cases.

CONCLUDING DISCUSSION

The Ames supersonic free-flight wind tunnel, instrumented as described in the preceding discussion, has proved to be a useful and accurate means of measuring drag coefficient. In one test program, the drag coefficient of 32 identical cone-cylinder models was measured over a wide range of Mach numbers. The mean scatter of these measurements was 1.2 percent from the faired curve. The drag as computed from theory agreed with the experimental measurements within 3 percent for all conditions. Consistency of measurements comparable to this has been obtained with other test bodies as well.

The tunnel is being used for studies of wave drag, base drag, boundary-layer transition, pitching moment, lift, and center of pressure, using the same shadowgraph-chronograph instruments as used for total-drag measurements.

The experience gained in the development and operation of the tunnel instrumentation indicates several possible improvements which could be incorporated to advantage in any subsequent installation of a similar type. Some of these improvements are listed below:

1. A divergent rather than a collimated shadowgraph light could be used, eliminating the initial expense and the necessary critical adjustment of the collimating mirrors. Compensation for the effects of the divergent light on the distance measurement would be made by using an auxiliary shadowgraph station at right angles to and operated simultaneously with the main shadowgraph station. The auxiliary station would record the position of the model along the optical axis of the main shadowgraph station.

2. A spark gap and condenser unit designed for minimum self-inductance could be used to provide shorter duration shadowgraph exposures.

3. The addition of an electronic circuit to automatically set the time delays would simplify operations. This could be performed by an additional photobeam station ahead of station number 1 which in

conjunction with station number 1 would ascertain the model velocity and, through associated circuits, set all the shadowgraph time delays.

4. A system to provide more positive triggering of the spark gap when the photobeam is interrupted by a model with a long slender nose would be desirable. If the model has a blunt base, this could be done by using the reversed polarity of the differentiated phototube signal to initiate the operation of the time delay when the base of the model leaves the photobeam.

Ames Aeronautical Laboratory,
National Advisory Committee for Aeronautics,
Moffett Field, Calif.

APPENDIX

INTERPOLATED COUNTER CHRONOGRAPH

The electronic chronograph is illustrated in the block diagram (fig.19). It consists of a counter chronograph (a Potter Instrument Company Model 450) and an interpolating oscilloscope.

The Counter Chronograph

A crystal controlled oscillator produces a 1.6-megacycle sinusoidal voltage which is coupled to an on-off gate circuit. Upon the arrival of an electrical pulse to the start terminal of the gate circuit, the 1.6-megacycle voltage is applied to the counters which count the number of complete cycles occurring before the 1.6-megacycle voltage is disconnected (by an electrical pulse arriving at the stop terminal).

The time during which the gate delivers a signal to the counters is the product of the oscillator period and the number of counts. This measurement has a definition of approximately ±1 microsecond.

The Interpolating Oscilloscope

A 100-kc oscillator drives the deflecting amplifiers of an interpolating oscilloscope. A 90° phase difference between the signals on the horizontal and vertical deflecting plates is obtained by use of a phase shift network; thus, the cathode-ray-tube electron beam describes a circle, one revolution being completed in 10 microseconds. A knowledge of the position of the beam at the instants of occurrence of start and stop pulses will provide a measurement of the time increments necessary to extend the definition of the counter chronograph record. A start or stop pulse arriving at the terminals of the counter chronograph is also applied to the Z-axis grid of the cathode ray tube to increase the intensity of the beam for the duration of the pulse. Thus a bright spot appears on the periphery of the circle, the angular position of which is determined by the phase of the oscillator signal at the instant of arrival of the pulse.

In order to distinguish between start and stop pulses the gain of the deflecting amplifiers is decreased by the radius change circuit after the start pulse arrives. The stop pulse is then presented on a smaller circle concentric with that upon which the start pulse appears.

The oscilloscope presentation is photographed. The reading of the counter chronograph is taken to determine the number of whole revolutions of the electron beam. The angular displacement, in fractions of a revolution, of the start pulse from the stop pulse in the direction of rotation of the electron beam provides the increment to be added to the counter-chronograph reading. The over-all accuracy of the measurement is approximately 0.05 microsecond.

Discussion

A more accurate instrument can be made by increasing the rate of rotation of the electron beam. The maximum rate utilized, however, must not exceed the definition of the counter chronograph or ambiguities in the over-all reading in units of the counter chronograph accuracy will be introduced.

The instrument described is limited to the measurement of a single time interval. To measure more than one time interval it is necessary to add more counter chronographs and to modify the radius change circuit so that the number of radii is equal to the number of stations being used in the wind tunnel. The instrument being developed will have four radii and will use three counter chronographs.

REFERENCES

1. Seiff, Alvin, James, Carlton S., Canning, Thomas N., and Boissevain, Alfred G.: The Ames Supersonic Free-Flight Wind Tunnel. NACA RM A52A24, 1952.

2. Jenkins, Francis A., and White, Harvey E.: Fundamentals of Physical Optics. McGraw-Hill Book Company, Inc., N.Y., 1937, pp. 436-437.

3. Schmidt, Stanley F., Briggs, Robert O., and Looschen, Floyd W.: Use of High-Pressure Mercury Arc Lamps for Pulsed-Light Applications. American Institute of Electrical Engineers miscellaneous paper, No. 50-183, May 1950.

4. Loeb, Leonard B.: Atomic Structure. John Wiley and Sons., Inc., N.Y., 1938, pp. 261-264.

TABLE I.- DESCRIPTION OF COMPONENTS IN FIGURE 9

Resistors

R1	10 M, 1/2 watt, carbon	R22	560 k, 1/2 watt, carbon
R2	220 k, 1/2 watt, carbon	R23	10 M, 1/2 watt, carbon
R3	47 k, 1 watt, carbon	R24	50 k, 2 watts, wire
R4	1 k, 1/2 watt, carbon	R25	470 k, 1/2 watt, carbon
R5	220 k, 1/2 watt, carbon	R26	47 k, 2 watts, carbon
R6	4.7 k, 1/2 watt, carbon	R27	470 k, 1/2 watt, carbon
R7	10 M, 1/2 watt, carbon	R28	100 ohm, 5 watts, wire
R8	1 M, 1/2 watt, carbon	R29	100 ohm, 5 watts, wire
R9	2.2 k, 1/2 watt, carbon	R30	470 k, 1/2 watt, carbon
R10	47 k, 1/2 watt, carbon	R31	2.2 M, 1/2 watt, carbon
R11	1 M, 1/2 watt, carbon	R32	33 k, 1 watt, carbon
R12	47 k, 2 watts, carbon	R33	10 k, 1 watt, carbon
R13	4.7 k, 1/2 watt, carbon	R34	81 k, 2 watts, carbon
R14	1 M, 1/2 watt, carbon	R35	1 M, 1/2 watt, carbon
R15	20 k, 10 watts, wire	R36	10 k, 5 watts, wire
R16	10 k, 1/2 watt, carbon	R37	300 k, 1/2 watt, carbon
R17	33 k, 1/2 watt, carbon	R38	100 k, 1/2 watt, carbon
R18	250 k, 1/2 watt, carbon	R39	10 k, 5 watts, wire
R19	470 k, 1/2 watt, carbon	R40	20 k, 2 watts, carbon
R20	47 k, 2 watts, carbon	R41	1 M, 1/2 watt, carbon
R21	470 k, 1/2 watt, carbon	R42	800 k, 4 watts, high voltage

Condensers

C1	.1 mfd, paper	C15	.09 mfd, paper
C2	20 mfd, electrolytic	C16	.01 mfd, paper
C3	25 mfd, electrolytic	C17	.1 mfd, paper
C4	.003 mfd, paper	C18	2 mfd, paper
C5	.0005 mfd, paper	C19	2 mfd, paper
C6	.01 mfd, paper	C20	.001 mfd, paper
C7	.0005 mfd, paper	C21	.15 mfd, paper
C8	20 mfd, electrolytic	C22	.15 mfd, paper
C9	.0005 mfd, paper	C23	25 mfd, electrolytic
C10	.008 mfd, paper	C24	.001 mfd, paper
C11	8 mfd, electrolytic	C25	.001 mfd, paper
C12	.1 mfd, paper	C26	.0005 mfd, paper
C13	.1 mfd, paper	C27	.1 mfd, pyranol
C14	.1 mfd, paper	C28	.001 mfd, glass mike

Note

k = 10^3 ohms
M = 10^6 ohms
mfd = microfarad

TABLE I.- CONCLUDED

Tubes

V1	922 phototube	V7	2050
V2	6SJ7	V8	2050
V3	6SN7	V9	6SN7
V4	6SN7	V10	6SN7
V5	6J7	V11	NE-2
V6	6J7		

Potentiometers

P1	70 k, wire-wound, 4 watts	P3	50 k, wire-wound, 4 watts
P2	70 k, wire-wound, 4 watts		

Transformers

T1	Automobile ignition coil	T2	Automobile ignition coil

TABLE II.- DESCRIPTION OF COMPONENTS IN FIGURE 16

Resistors

R1	5 k, 2 watts, carbon	R11	.2 M, 1 watt, carbon
R2	5 k, 2 watts, carbon	R12	50 k, 1 watt, carbon
R3	39 k, 2 watts, carbon	R13	.2 M, 1 watt, carbon
R4	39 k, 2 watts, carbon	R14	40 k, 2 watts, carbon
R5	.2 M, 1 watt, carbon	R15	5 k, 25 watts, wire
R6	.2 M, 1 watt, carbon	R16	.1 M, 2 watts, carbon
R7	50 k, 1 watt, carbon	R17	.1 M, 2 watts, carbon
R8	10 k, 2 watts, carbon	R18	1 k, 10 watts, wire
R9	.2 M, 1 watt, carbon	R19	300 ohms, 150 watts, wire
R10	50 k, 1 watt, carbon	R20	750 ohms, 200 watts, wire

Condensers

C1	.01 mfd, 500 v, paper	C8	.1 mfd, 500 v, paper
C2	.1 mfd, 500 v, paper	C9	.5 mfd, 1000 v, paper
C3	.005 mfd, 500 v, paper	C10	16 mfd, 500 v, electrolytic
C4	.01 mfd, 500 v, paper		
C5	.01 mfd, 500 v, paper	C11	.005 mfd, 1000 v, mica
C6	.1 mfd, 500 v, paper	C12	.005 mfd, 500 v, mica
C7	.05 mfd, 500 v, paper	C13	.1 mfd, 500 v, paper

Tubes

V1	2050	V4	5881
V2	2050	V5	VR75
V3	2050	V6	35T

Relays

RY1 D.P.D.T. relay

RY2 D.P.D.T. high-voltage relay

Note

k = 10^3 ohms
M = 10^6 ohms
mfd = microfarad

TABLE III.- DESCRIPTION OF COMPONENTS IN FIGURE 17

Resistors

R1	20 k, 2 watts, carbon	R4	10 k, 100 watts, wire
R2	20 k, 2 watts, carbon	R5	25 k, 25 watts, wire
R3	5 k, 1 watt, carbon	R6	5 k, 200 watts, wire

Condensers

C1	.001 mfd, mica	C8	.05 mfd, mica
C2	.01 mfd, mica	C9	.01 mfd, mica
C3	.001 mfd, mica	C10	12 mmfd (section of RG-8-U coax)
C4	10 mmfd, mica		
C5	100 mmfd, mica	C11	1200 mmfd, mica
C6	.05 mfd, paper	C12	1 mfd, paper
C7	.01 mfd, mica	C13	1 mfd, paper

Inductors

L1	2.5 mh, 150 ma	L3	2.5 mh, 1 amp
L2	2.5 mh, 150 ma	L4	2.5 mh, 1 amp

Tubes

V1	6AL5	V4	4-250A
V2	814	V5	2X2
V3	4-250A		

Miscellaneous

PS	parasitic suppressor	MA	milliammeter
MJ	monitor jack	KV	kilovoltmeter

Note

k	= 10^3 ohms	mmfd	= micro-microfarad
M	= 10^6 ohms	mh	= millihenry
mfd	= microfarad	ma	= milliamps

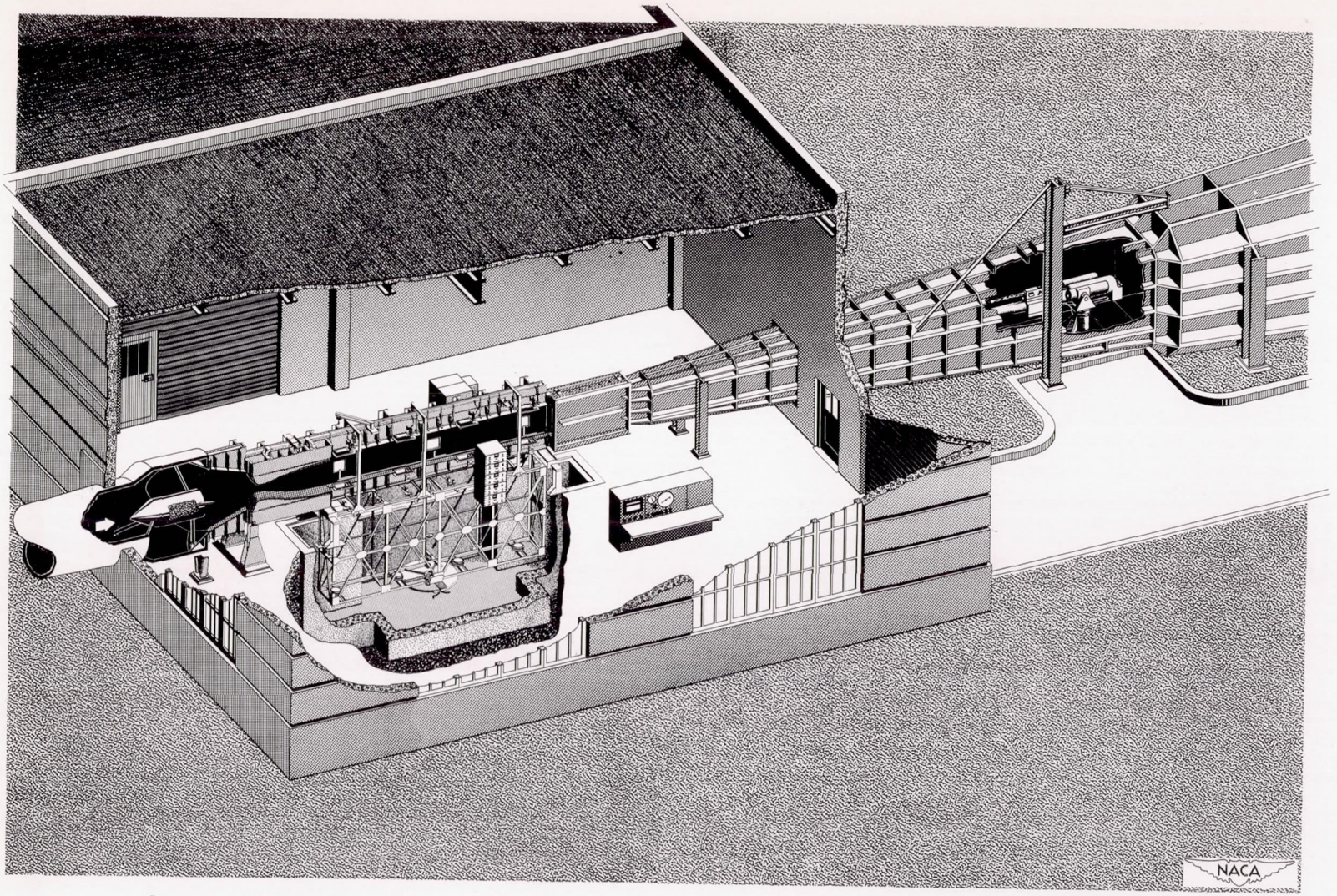

Figure 1.- General arrangement of the wind tunnel and associated equipment.

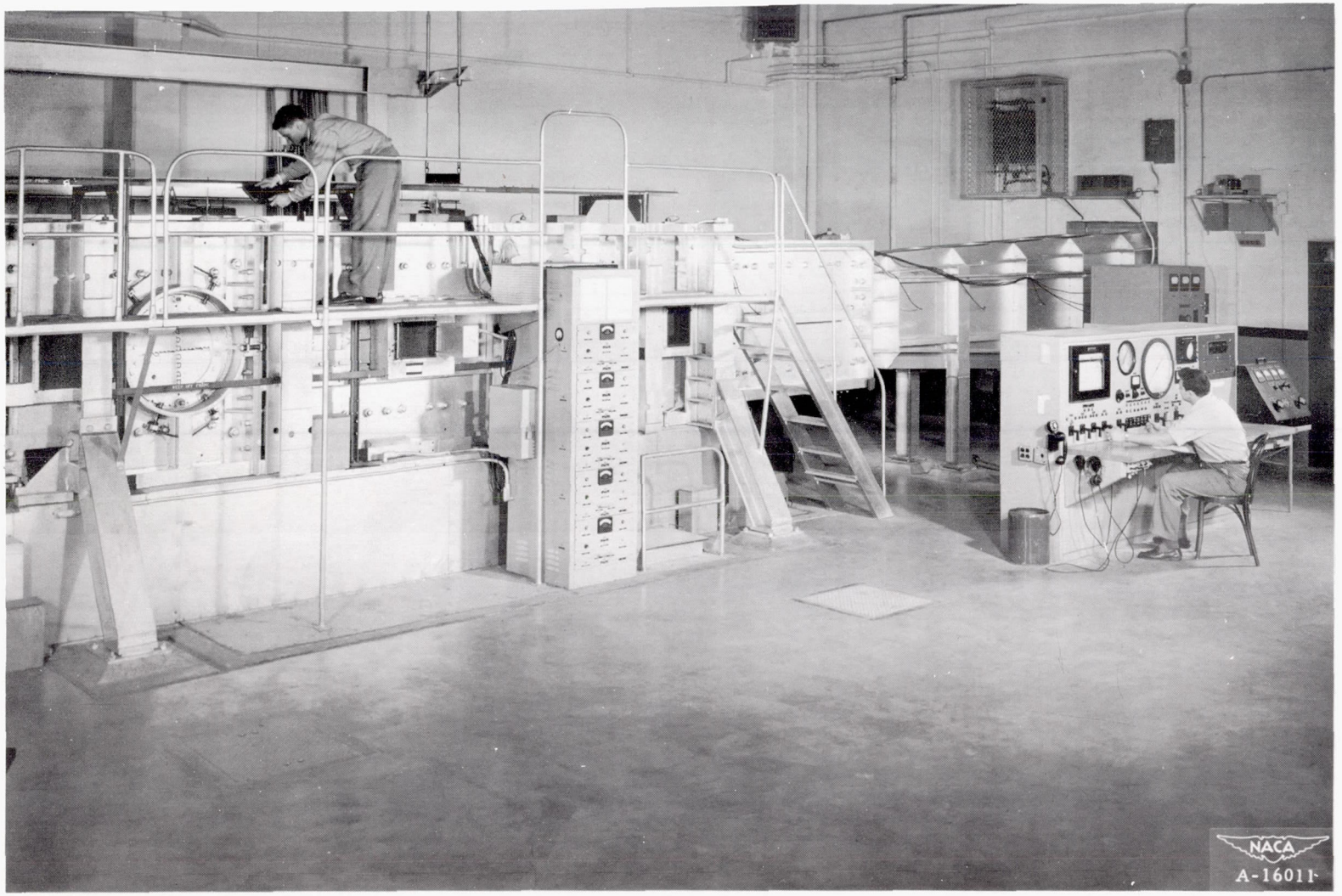

Figure 2.- Exterior of the test section, the control center, and the shadowgraph electronic equipment.

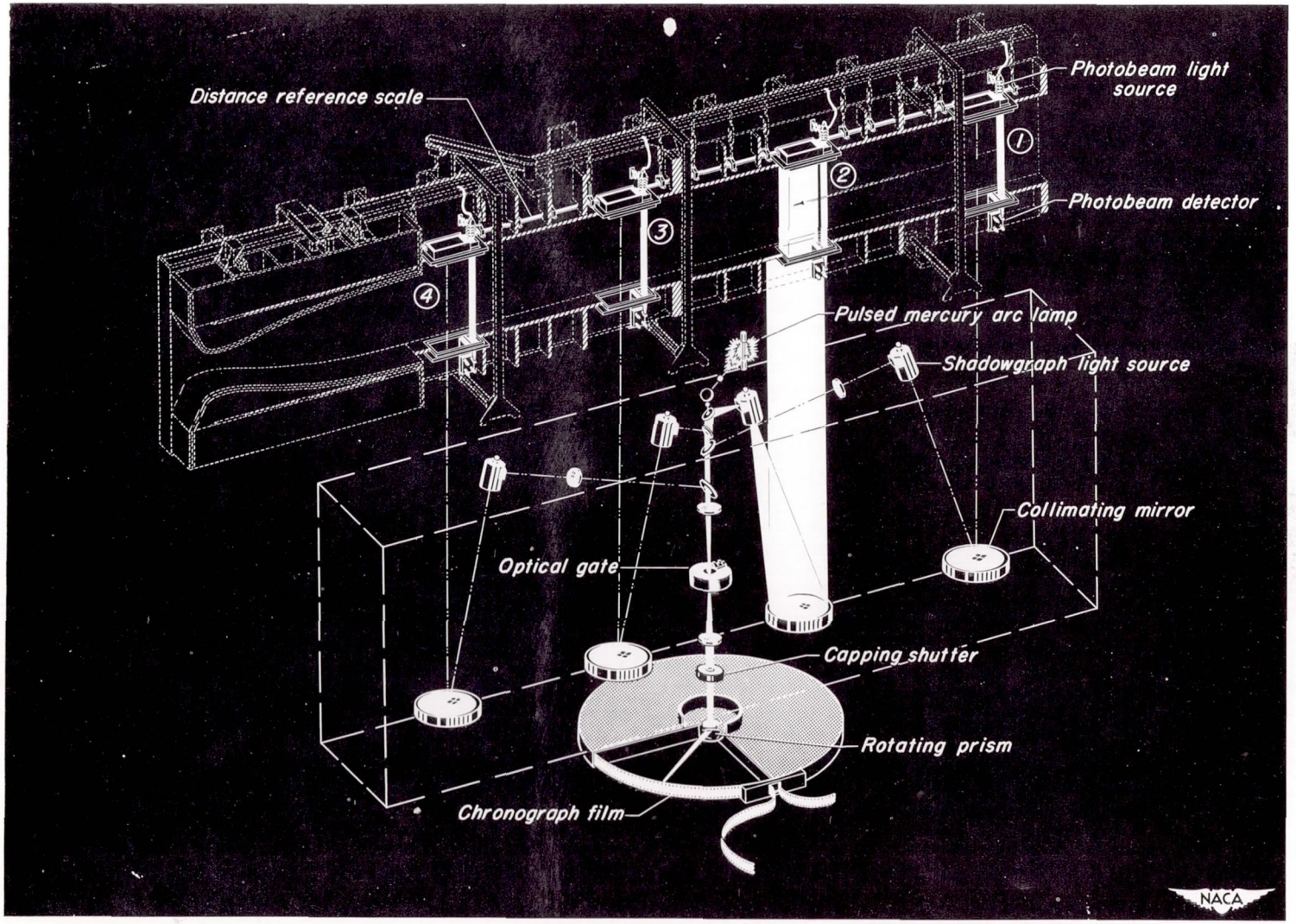

Figure 3.- Schematic drawing of the test section and optical components of the shadowgraph and chronograph equipment.

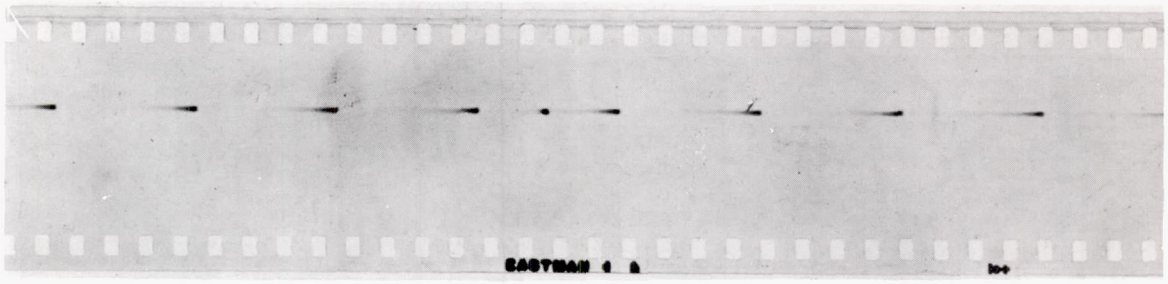

(a) Section of a chronograph record showing one station mark and timing marks recorded at 50,000 pulses per second.

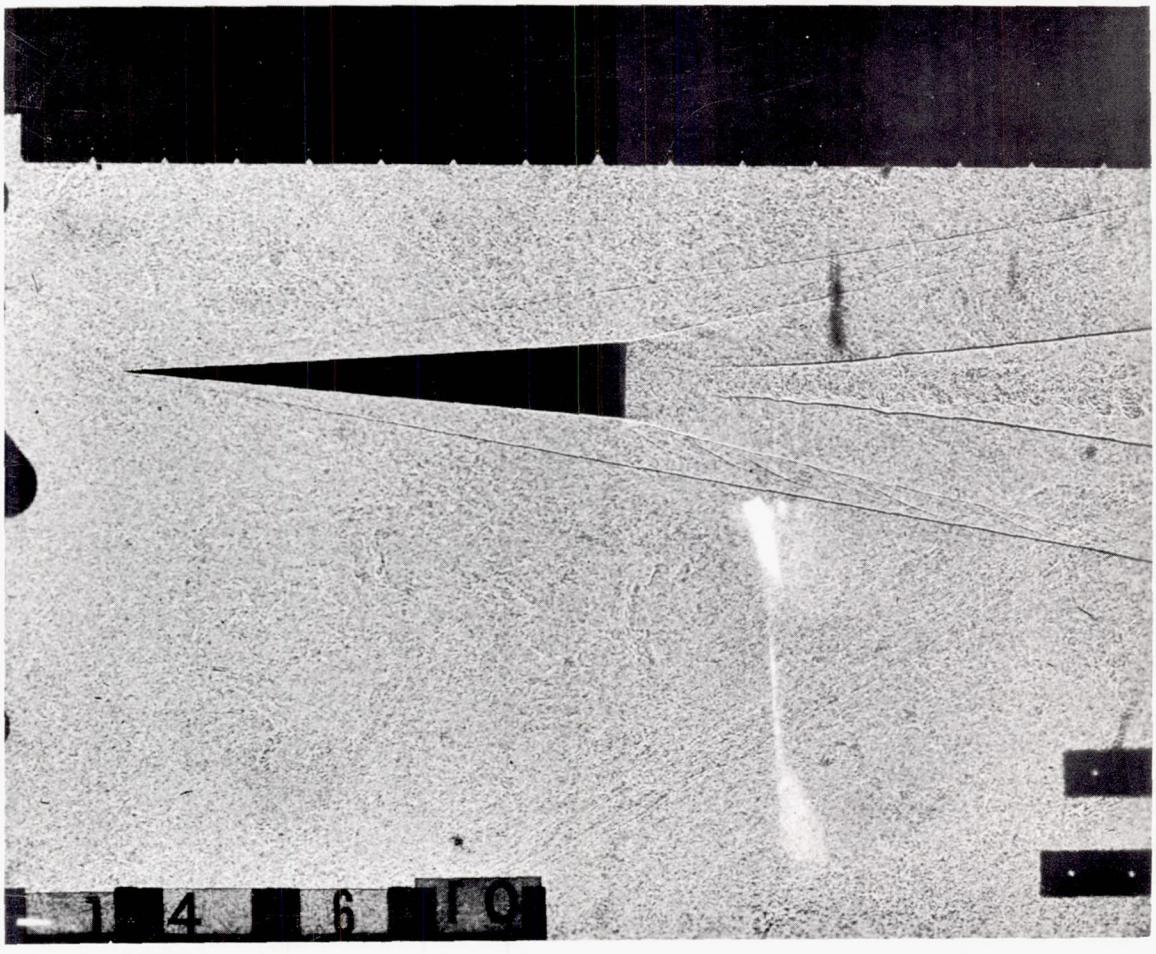

(b) Shadowgraph record of a model.

NACA
A-16265.1

Figure 4.- Records from the Ames supersonic free-flight wind tunnel.

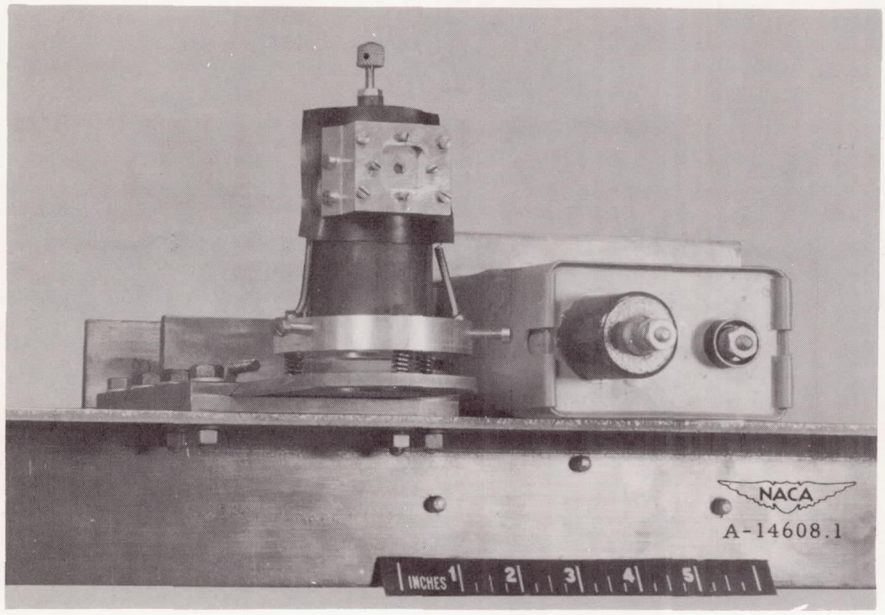

(a) Spark gap and condenser mounted on frame.

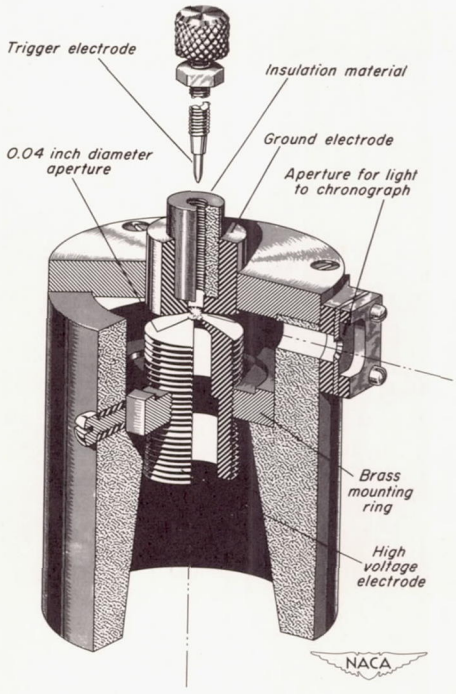

(b) Cutaway drawing of the spark gap.

Figure 5.- Spark gap used for shadowgraph light source.

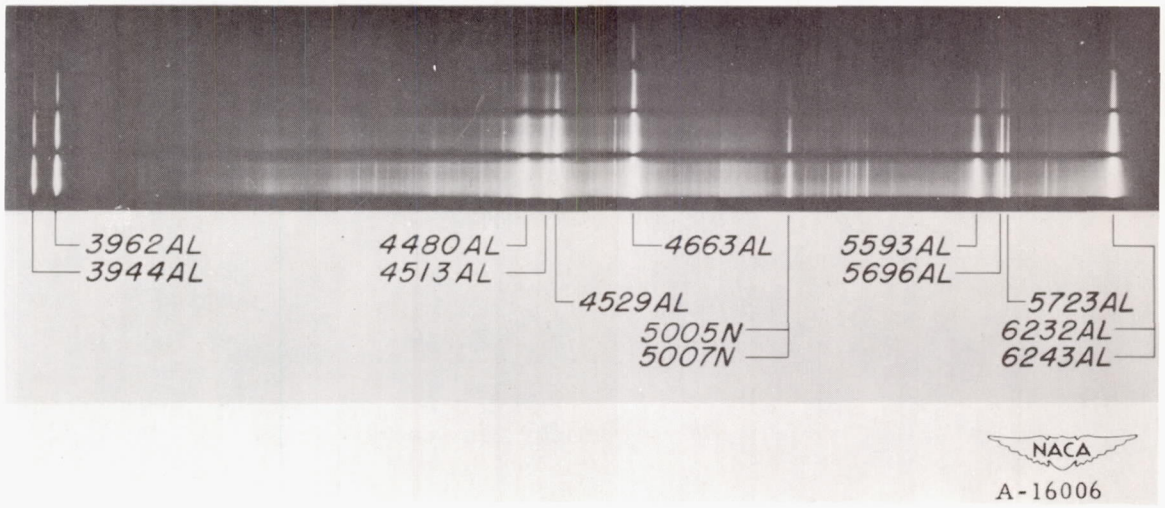

Figure 6.- Spectrogram of the shadowgraph light source.

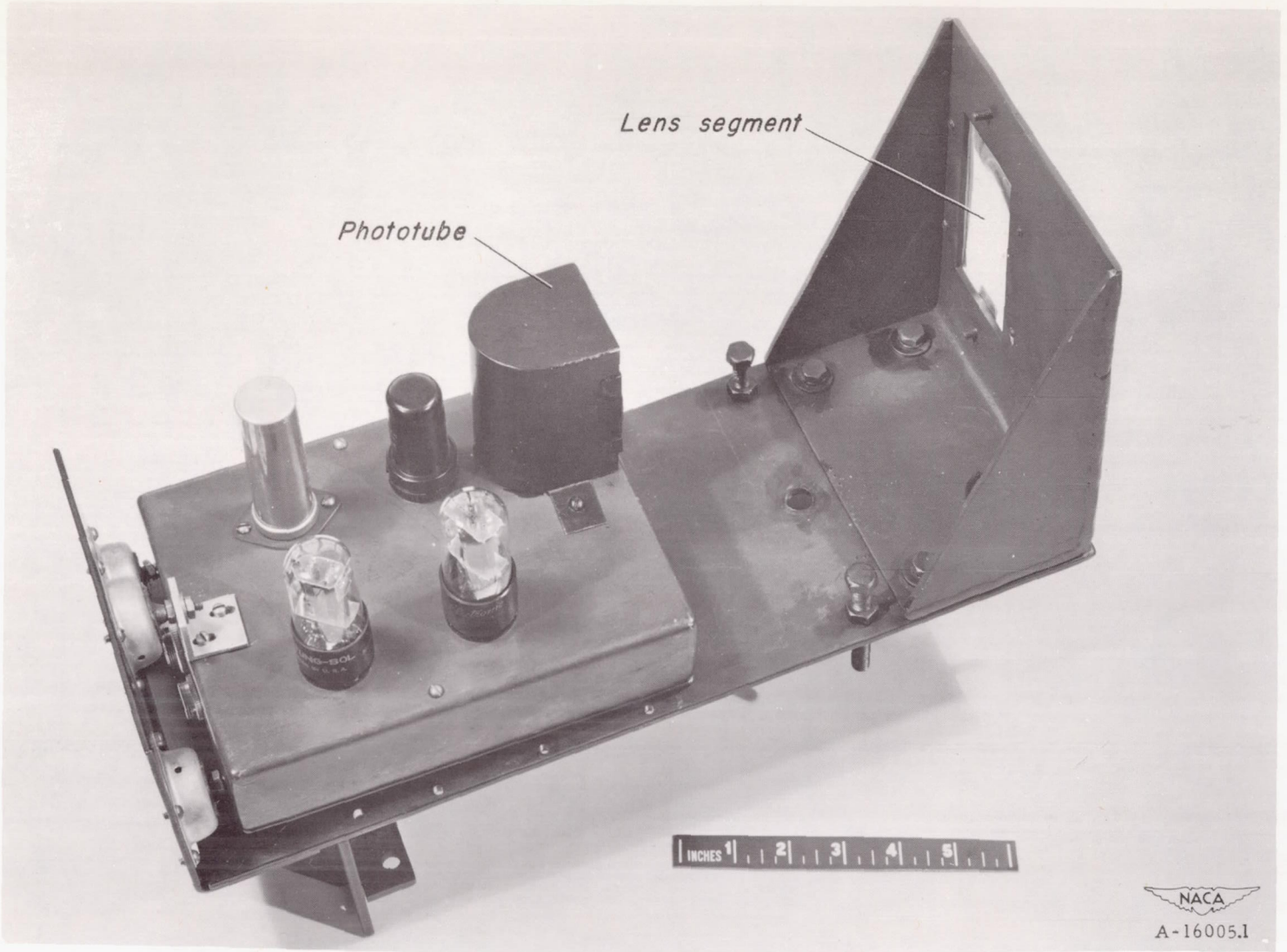

Figure 7.- Photobeam-detector chassis and rectangular lens segment.

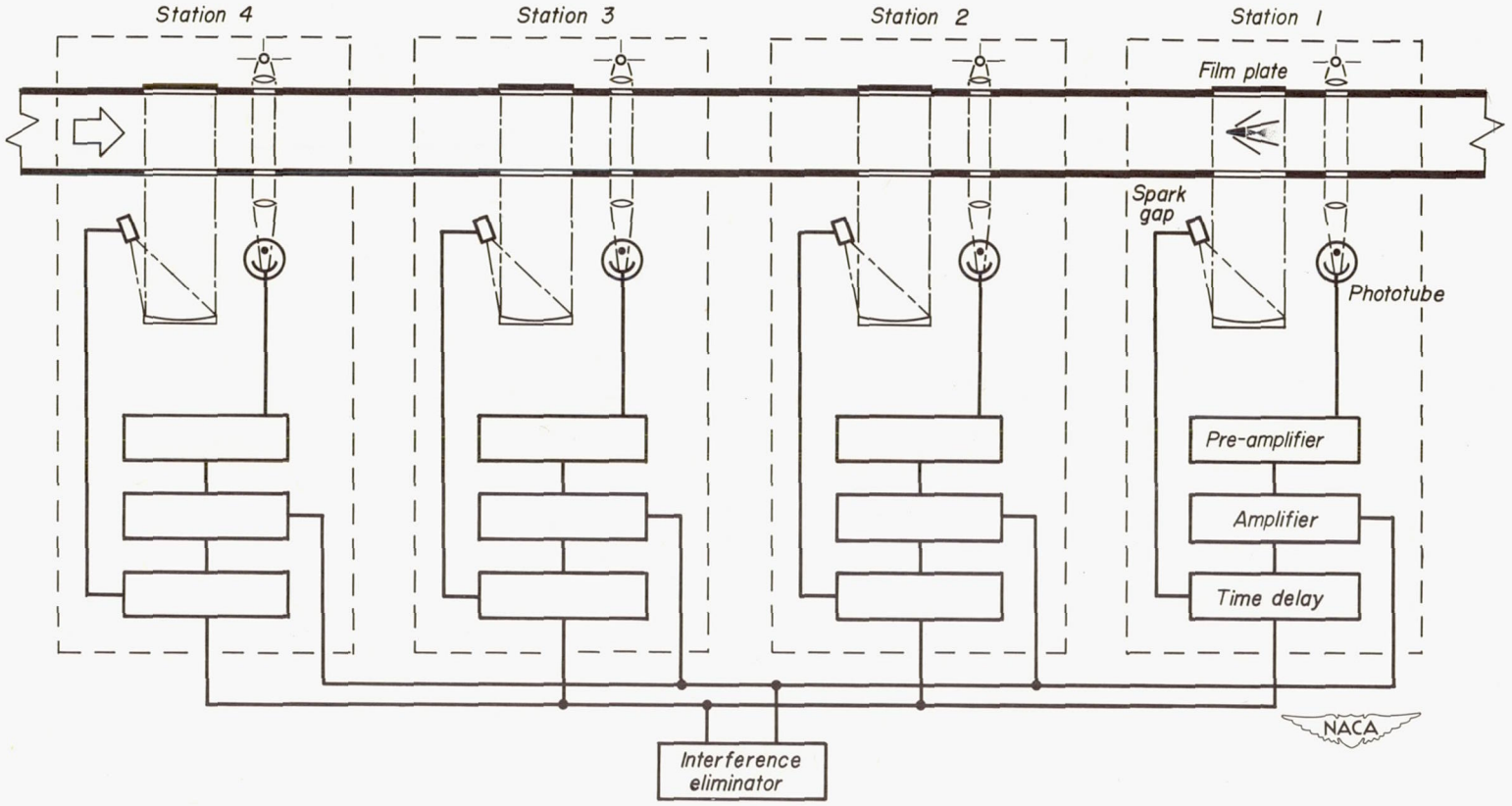

Figure 8.– Block diagram of the shadowgraph equipment.

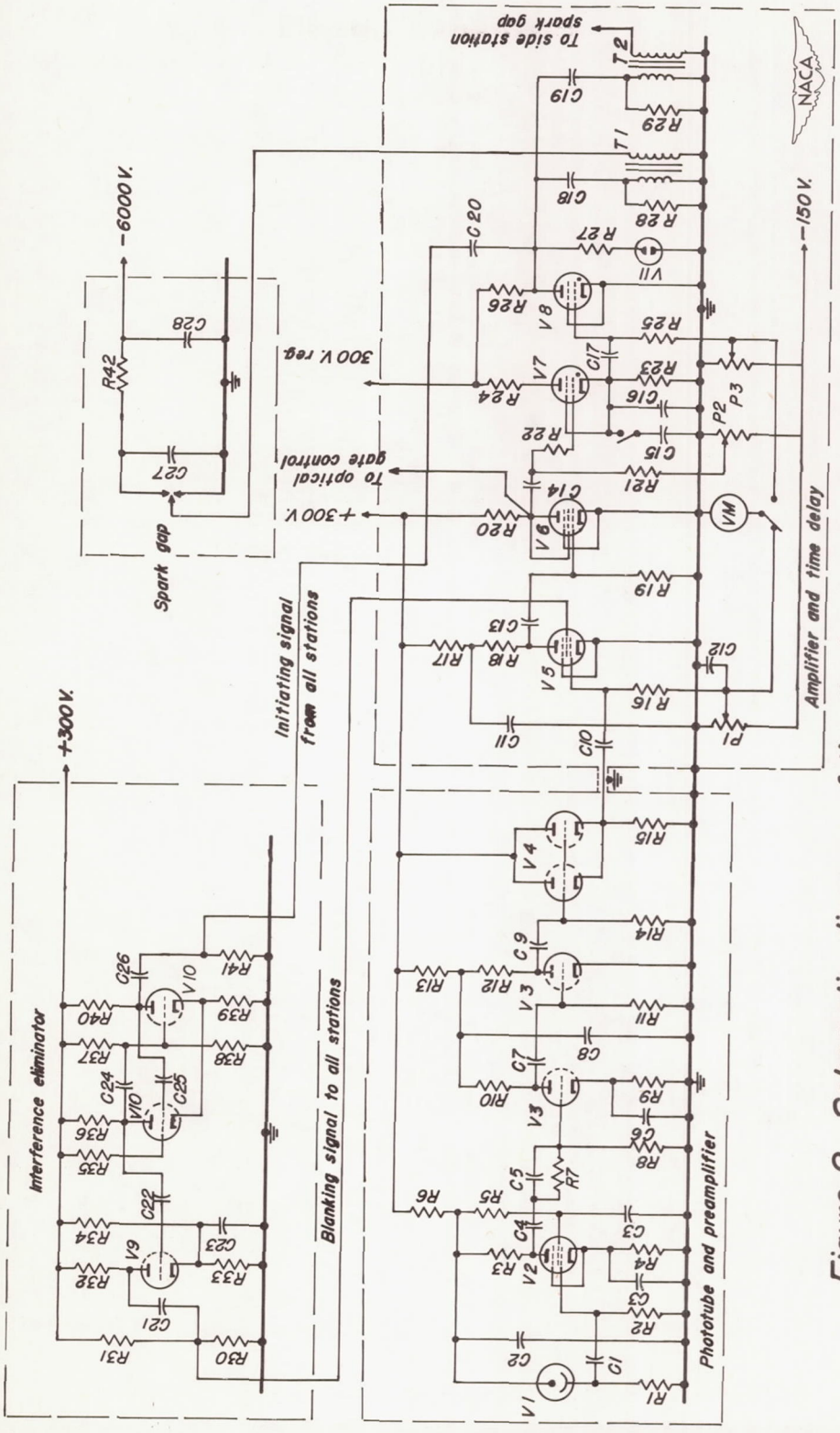

Figure 9.- Schematic diagram of the shadowgraph electronic equipment.

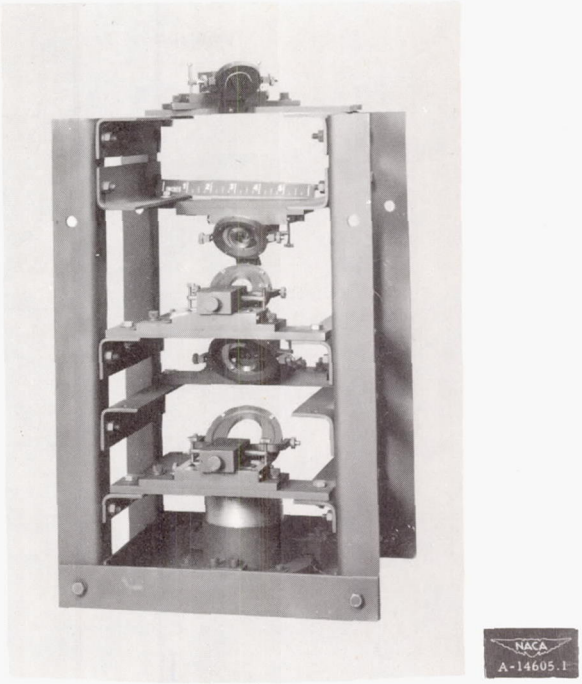

Figure 10.- Chronograph concentric-mirror assembly.

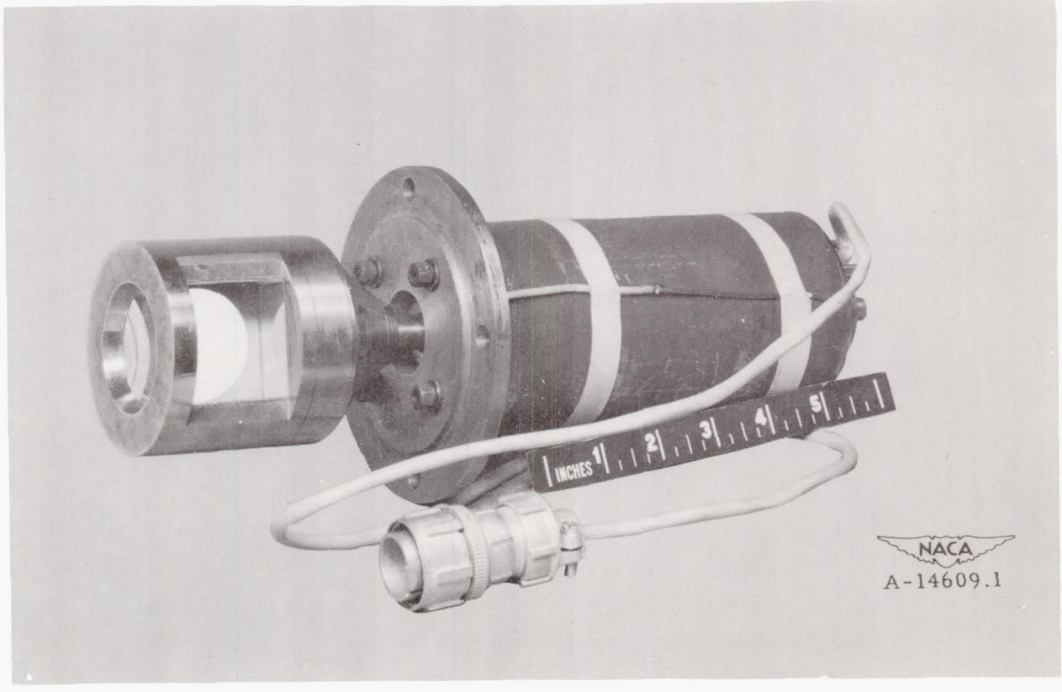

Figure 11.- Rotating-prism drive-motor assembly.

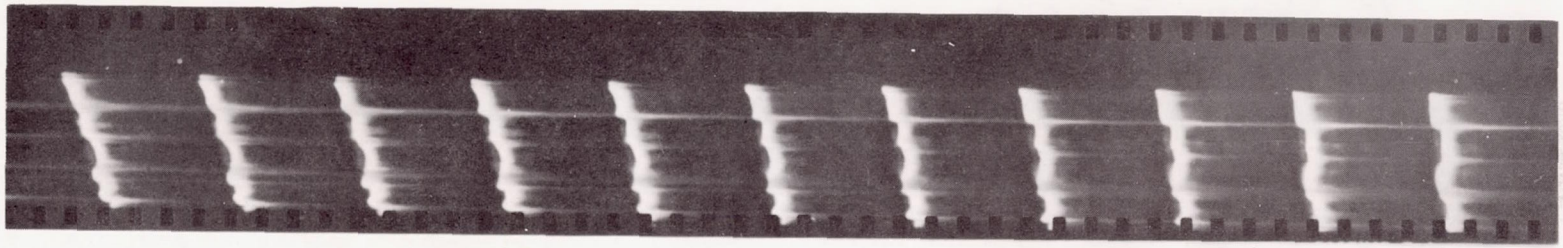

Figure 12.- Series of photographs of the arc within the BH-6 lamp under pulse operation at 100,000 pulses per second.

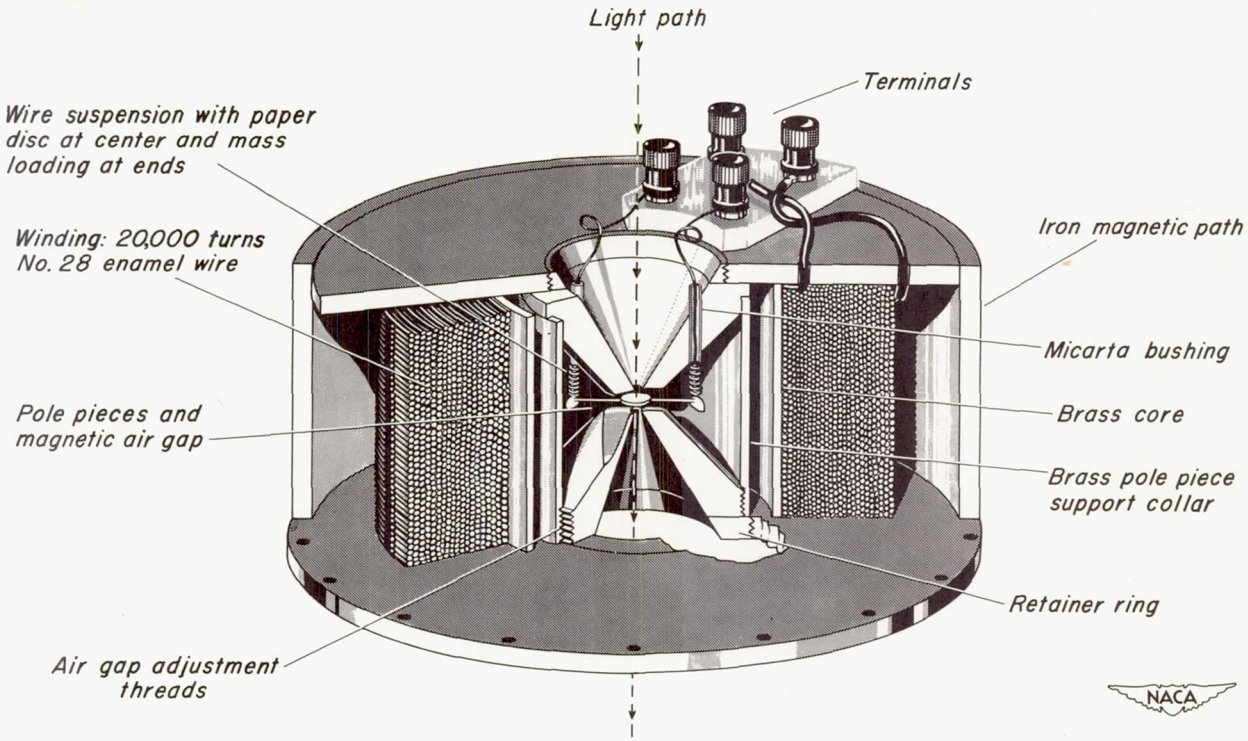

(a) Cutaway drawing of the optical gate.

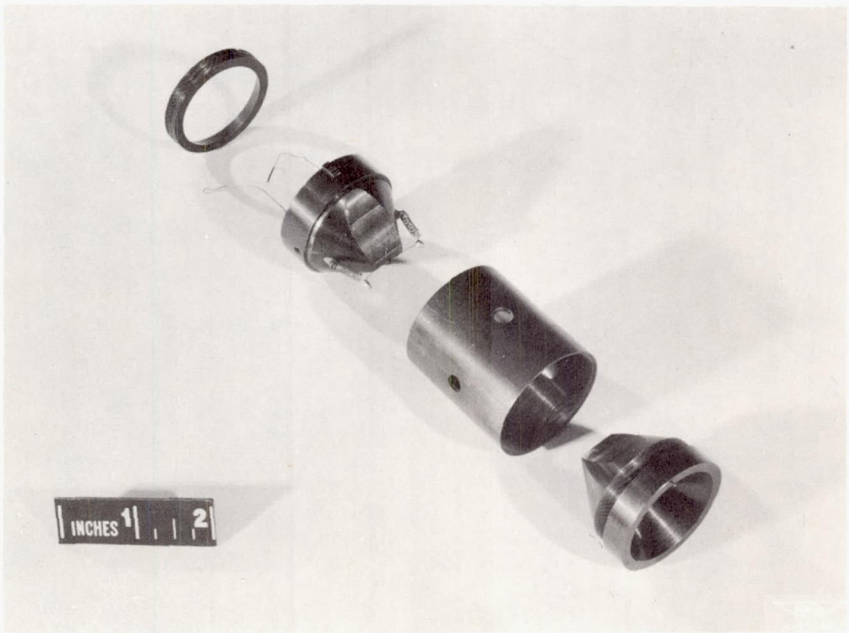

(b) Optical-gate pole pieces, support collar, retainer ring, and armature assembly.

Figure 13.- Optical gate.

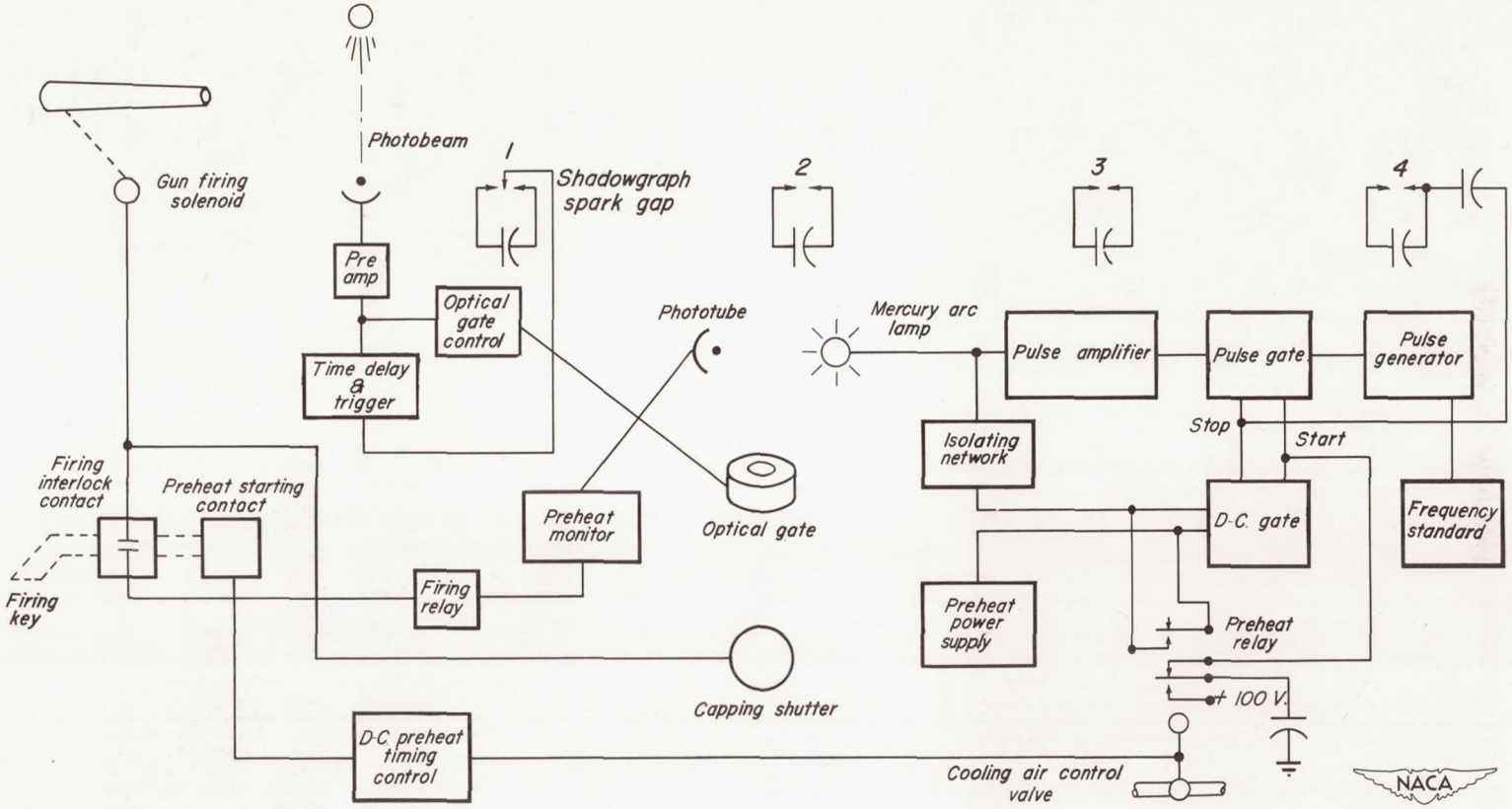

Figure 14.- Block diagram of the rotating prism chronograph.

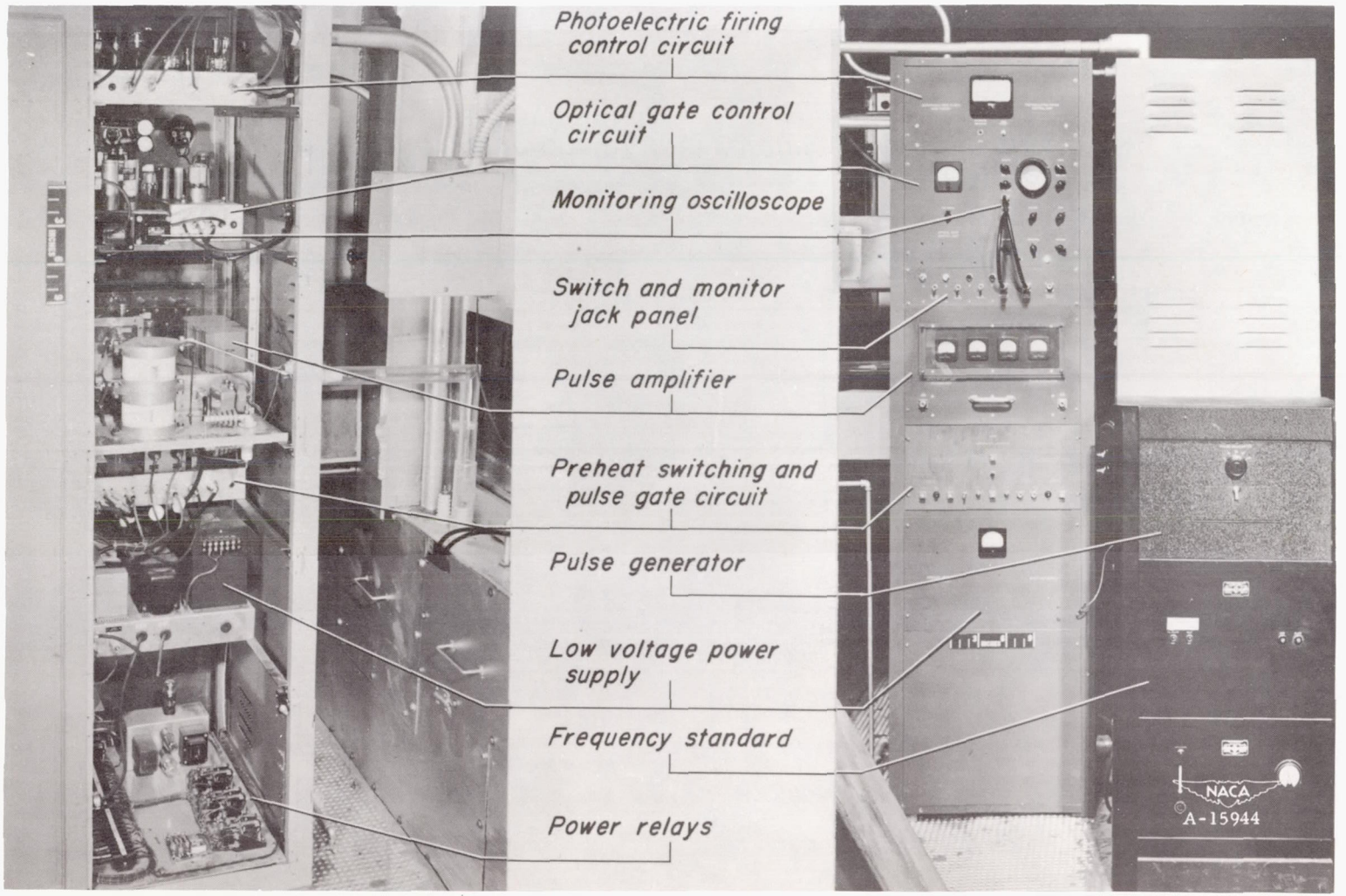

Figure 15.- The electronic equipment associated with the chronograph.

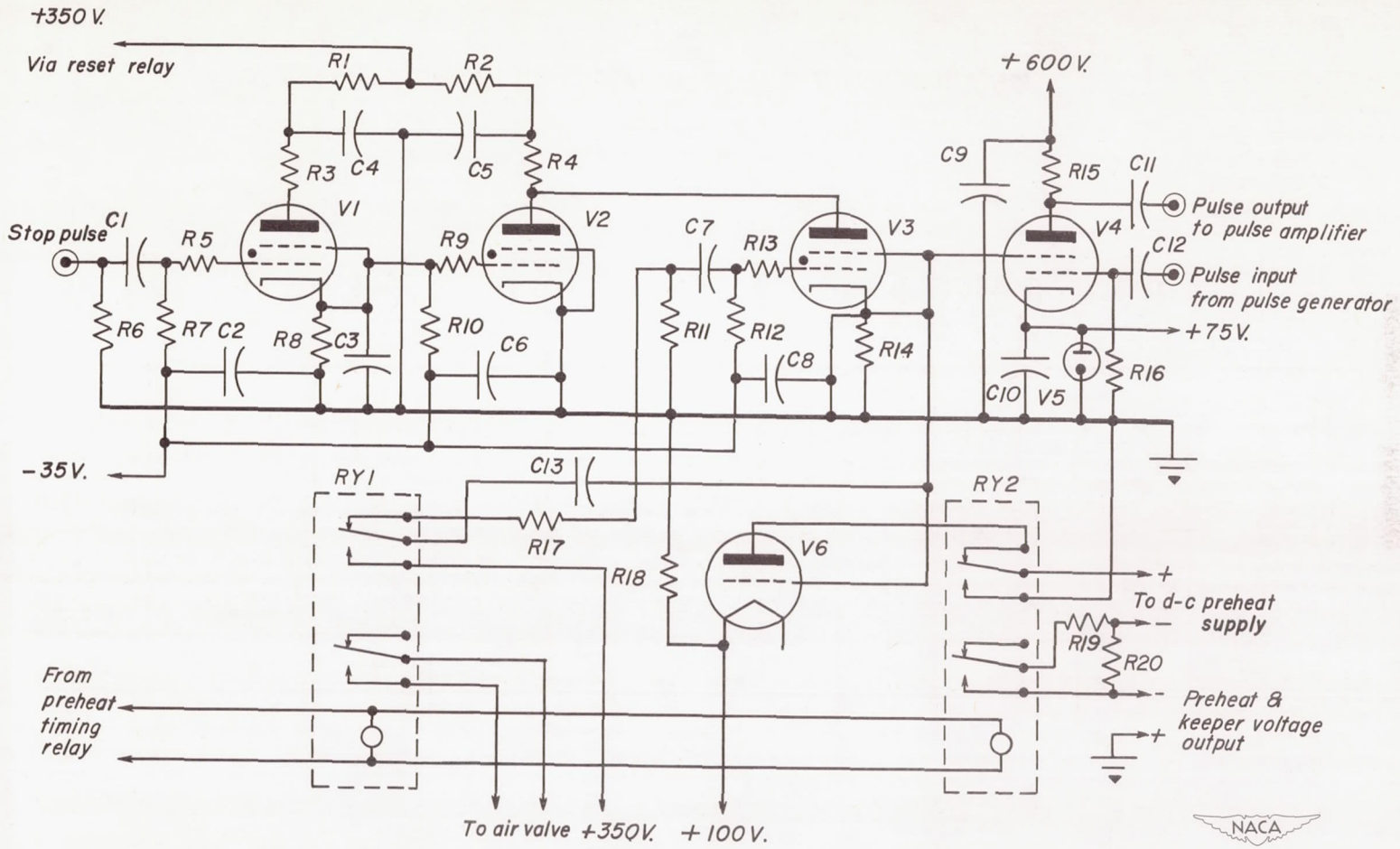

Figure 16.- Schematic diagram of the preheat switching and pulse gate circuits.

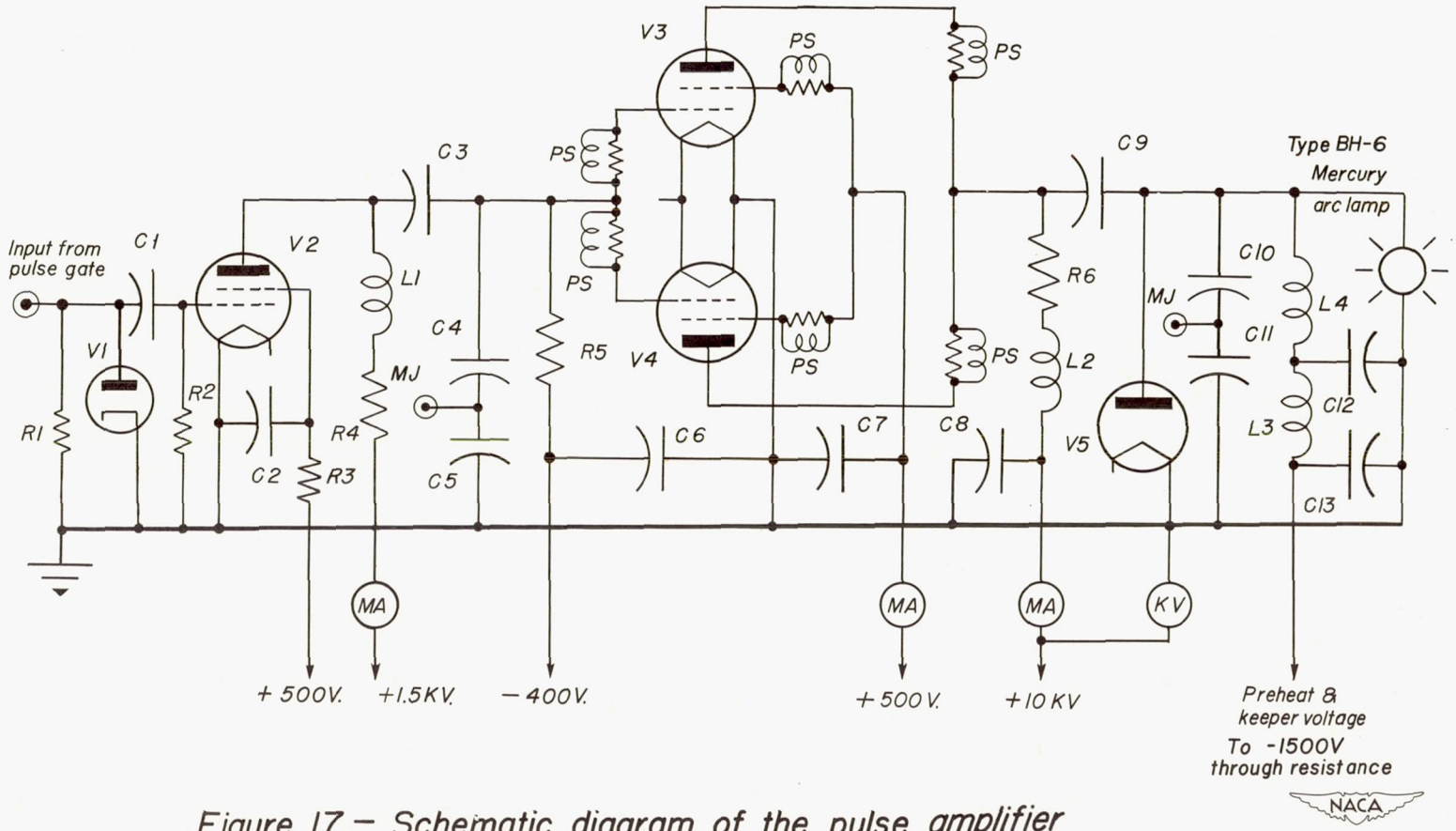

Figure 17.– Schematic diagram of the pulse amplifier.

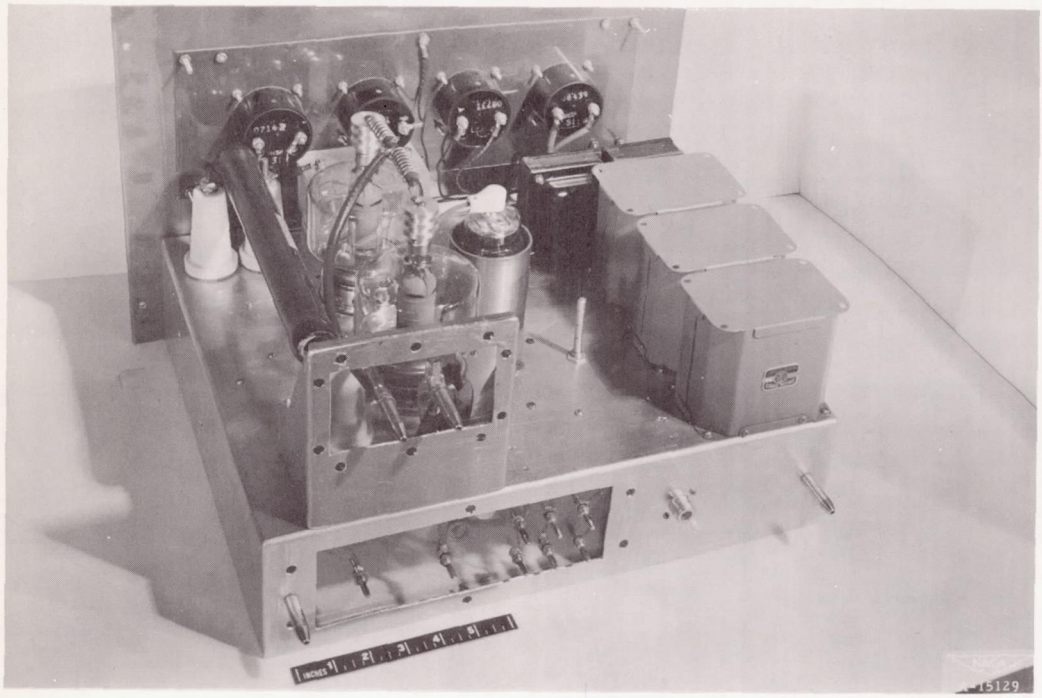

(a) Three-quarter top view of chassis.

NACA
A-15129

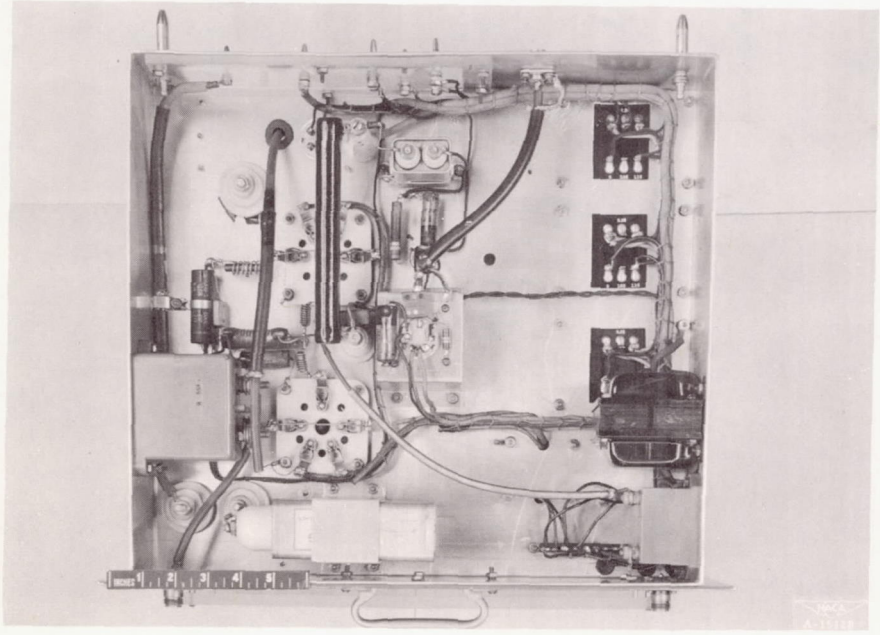

(b) Bottom view of chassis.

NACA
A-15128

Figure 18.- Pulse amplifier circuit.

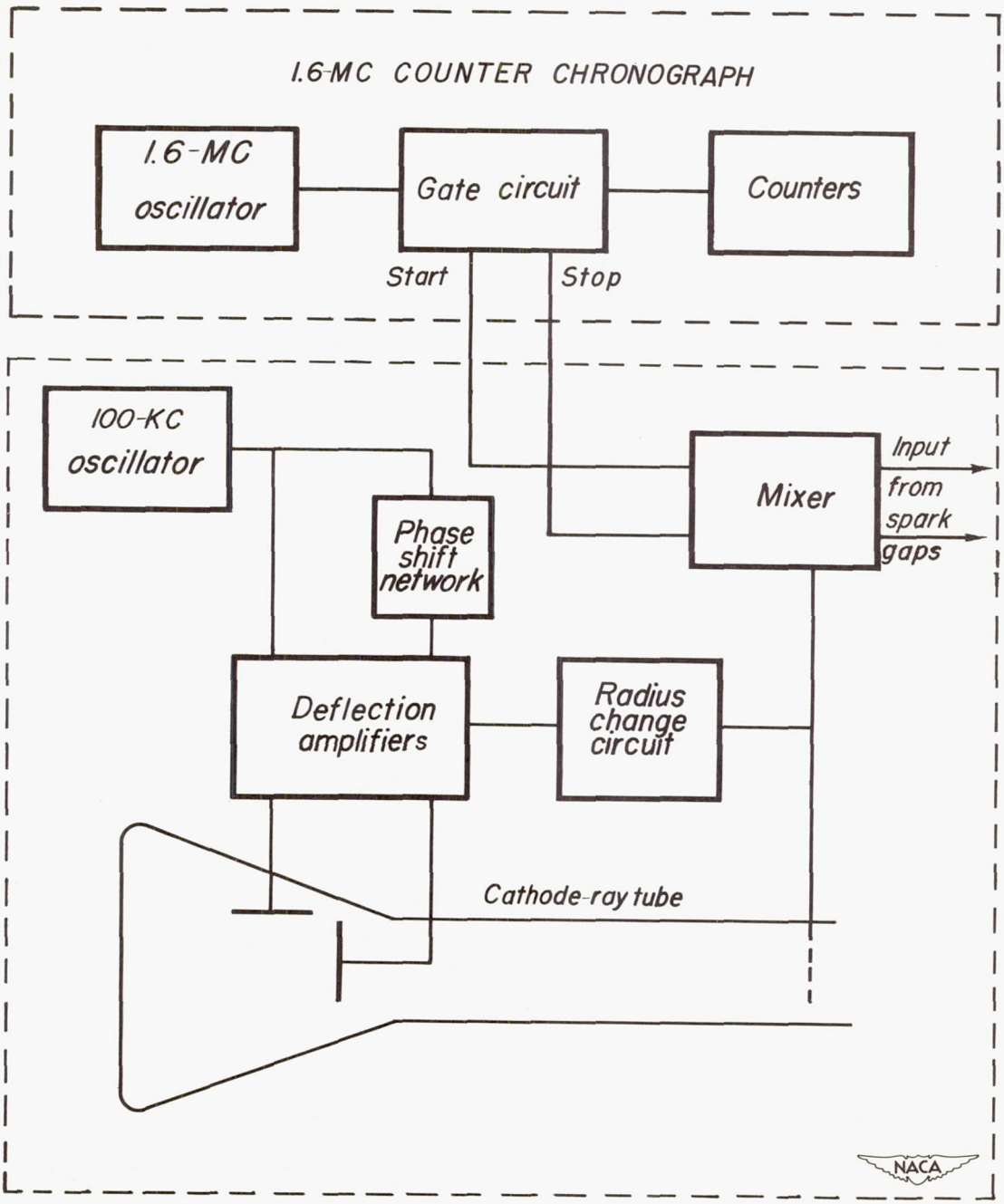

Figure 19.- Block diagram of the interpolated counter chronograph.